

AERONAUTICS LIBRARY
California Institute of Technology

GUGGENHEIM AERONAUTICAL LABORATORY

CALIFORNIA INSTITUTE OF TECHNOLOGY

THE LAW OF THE WAKE
IN THE TURBULENT BOUNDARY LAYER

Donald C^oles

PASADENA, CALIFORNIA

THE LAW OF THE WAKE
IN THE TURBULENT BOUNDARY LAYER

Donald Coles

Guggenheim Aeronautical Laboratory
California Institute of Technology
Pasadena

December 20, 1955

Abstract

After an extensive survey of mean-velocity profile measurements in various two-dimensional incompressible turbulent boundary-layer flows, it is proposed to represent the profile by a linear combination of two universal functions. One is the well-known law of the wall. The other, called the law of the wake, is epitomized by the profile at a point of separation or reattachment. These functions are considered to be established empirically, by a study of the mean-velocity profile, without reference to any assumed mechanism of turbulence. Using the resulting complete analytic representation for the mean-velocity field, the shear field is computed from the boundary-layer equations and compared with experimental data for several flows.

The state of a turbulent boundary layer is ultimately interpreted in terms of an equivalent wake profile, which supposedly represents the large-eddy structure and is a consequence of the constraint provided by inertia. This equivalent wake profile is modified by the presence of a wall, at which a further constraint is provided by viscosity. The wall constraint, although it penetrates the entire boundary layer, is manifested chiefly in the sublayer flow and in the logarithmic profile near the wall.

Finally, it is suggested that yawed or three-dimensional flows may be usefully represented by the same two universal functions, considered as vector rather than scalar quantities. If the wall component is defined to be in the direction of the surface shearing stress, then the wake component, at least in the few cases studied, is found to be very nearly parallel to the gradient of the pressure.

I. THE LAW OF THE WALL.

A. Historical Development.

1. Evolution before 1949. Consider a turbulent shear flow which is steady and two-dimensional on the average. Let $u(x, y)$ and $v(x, y)$ be the mean velocities in the direction of increasing rectangular coordinates x and y respectively. Suppose that the flow exerts a shearing stress $\tau_w(x)$ on a smooth impermeable wall at rest at $y = 0$. For a fluid of constant density, define a friction velocity $u_\tau(x)$ by

$$\rho u_\tau^2 = \tau_w \quad (1)$$

Under these conditions, experience with turbulent shear flow has been that the mean-velocity profile in a considerable region near the surface is described by a relationship called the law of the wall,

$$\frac{u}{u_\tau} = f\left(\frac{yu_\tau}{\nu}\right) \quad (2)$$

The earliest statement of this law, by Prandtl, von Kármán, and others, was based on a simple dimensional argument. Suppose that the mean-velocity profile is found to be adequately represented by a relationship $\varphi(u, y, \delta, \tau_w, \mu, \rho) = 0$, in an obvious notation, and that this relationship is found in some region to be independent of the characteristic length δ . It follows without any assumptions about the nature of the turbulence that u/u_τ in this region is necessarily a function of yu_τ/ν only.

Before the development of the mixing analogy the function in question was sometimes taken as a power law, for lack of a better representation. The sublayer, that is the region of predominantly viscous shear, was treated separately by assuming a linear velocity profile very near the wall; to this approximation $\partial u / \partial y = u / y = \tau / \mu = \tau_w / \mu = u_\tau^2 / \nu$, and therefore $u / u_\tau = y u_\tau / \nu$.

By 1930 the present general formulation of the law of the wall had been achieved, in the sense that no distinction was made in Eq. (2) between the sublayer and the fully turbulent flow. Nikuradse, at the suggestion of Prandtl, expressed the law of the wall in this sense during an analysis¹ of some measurements in pipe flow. Eq. (2) also appears in articles by Tollmien and by Schiller in Volume IV of Handbuch der Experimentalphysik.

At about the same time, the mixing analogy of Prandtl² and the similarity hypothesis of von Kármán³ had provided an equation $\partial u(x, y) / \partial y = u_\tau(x) / \kappa y$ for the mean velocity in the fully turbulent region, with the integral $u / u_\tau = (1/\kappa) \ln [y / y_0(x)] + \text{constant}$. It should be noted, however, that the choice of ν / u_τ for the unspecified characteristic length $y_0(x)$ is not properly a part of the mixing analogy, but rather a part of the dimensional argument already mentioned.

2. Recent Developments. Until quite recently, the three most important elements in the development of the law of the wall have been first, the dimensional argument implying Eq. (2); second, the stipulation that the function f is linear at the wall; and third, the recognition, for whatever reason, that the function f is very nearly logarithmic in a certain region outside the sublayer.

A fourth important element was contributed in 1949 by Ludwig and Tillmann⁴. By means of an ingenious heat-transfer technique for indirect measurement of surface shearing stress, they showed that the function f of Eq. (2) is apparently independent of pressure gradient for a wide range of experimental conditions.

This last observation lies at the heart of the present study, virtually every part of which depends directly or indirectly on the hypothesis that the law of the wall is a unique and universal relationship for flow past a smooth surface.

For the special case of steady two-dimensional incompressible flow, the form of the universal law is supposedly known. In particular, for values of $y u_\tau / \nu$ greater than about 50, Eq. (2) takes the form

$$\frac{u}{u_\tau} = \frac{1}{\kappa} \ln \frac{y u_\tau}{\nu} + c \quad (3)$$

where κ and c are constants to be determined experimentally.

For flow in a boundary layer, the general validity of Eq. (3) can be tested by observing, as have Clauser⁵ and others, that this expression is an implicit equation for u_τ , i.e. for τ_w , when ρ , μ , and $u(y)$ are given. The law of the wall thus provides a means for accurate determination of the elusive wall shearing stress, once the function f in Eq. (2) has been established by a survey of experimental data in flows for which the shear is accurately known.

3. Experimental Data. Nikuradse's classical pipe measurements¹ in 1930 confirmed the prediction of a logarithmic region in the mean-velocity profile. Fig. 1 shows the data obtained, including a small correction for wall interference, in sixteen surveys at various Reynolds

numbers of the region between the pipe wall and a value of y/r of about 0.15, where r is the pipe radius. Nikuradse did not obtain data in the sublayer, rather inferring the validity of the general law of the wall from the argument already given in favor of the limiting form $u/u_\tau = y u_\tau / \nu$ at $y = 0$. This omission was partly repaired in 1940 by Reichardt's measurements⁶ of mean velocity in the sublayer of a channel flow, and more completely repaired about 1953 by work of Laufer⁷ and Klebanoff⁸ in pipe flow and boundary-layer flow respectively.

The latter measurements, shown in Fig. 1, include data in the sublayer obtained in each instance with a hot-wire anemometer. For Laufer's experiments in pipe flow the wall shearing stress has been derived from the observed axial pressure gradient. For Klebanoff's experiments in a boundary layer the wall shearing stress has been derived from the rate of momentum loss observed in other experiments with the same model^{9,10}. For Reichardt's experiments in channel flow the wall shearing stress was not measured independently, as Reichardt's object was to interpolate experimentally in the region of the mean-velocity profile not studied by Nikuradse.

Finally, some measurements by Sheppard¹¹ in a natural wind near the ground offer a striking example of a boundary-layer flow for which it would seem that no Reynolds number can be explicitly defined. However, difficulty in visualizing either an origin of coordinates or a second boundary does not prevent the presentation of these data in terms of the law of the wall. Sheppard observed the surface shearing stress directly, using the floating-element technique, together with the mean velocity at several points up to a height of two meters. The

result of the measurements is given in Fig. 1. The agreement with wind-tunnel data is surprisingly good when it is considered that Sheppard's measurements were made over a concrete surface, and that the vertical temperature gradient may have differed significantly from the adiabatic lapse rate associated with neutral stability.

4. Numerical Evaluation. Two empirical constants, κ and C , appear in Eq. (3). Throughout the present study, the numerical values given to these constants are

$$\kappa = 0.40$$

$$C = 5.1$$

A great variety of other values, especially for κ , can be found in the experimental literature. However, in all cases where Eq. (3) is explicitly taken as a definition, κ is found to lie between 0.39 and 0.41. Values outside this range are usually the result of operations or assumptions which change the sense of the definition. In any event, it is clear in Fig. 1 that the data outside the sublayer are well represented by Eq. (3) when κ and C are given the values already mentioned.

Within the sublayer, on the other hand, large fluctuations in velocity and cramped quarters for experimentation usually combine to make measurements of mean velocity somewhat uncertain. The available data in Fig. 1 therefore should not be said to establish conclusively the uniqueness of the law of the wall in the sublayer, although these data have been used elsewhere¹² in forming a tentative estimate of the function $f(yu_{\tau}/\nu)$ and related functions.

B. Test of the Wall Law.

1. Momentum Balance. Except for a few applications of the floating-element technique in flows at constant pressure, values of surface shearing stress in turbulent boundary layers have usually been obtained indirectly from the observed pressure gradient and rate of momentum loss, using the momentum-integral equation of von Kármán¹³. For two-dimensional incompressible steady mean flow in a boundary layer, this equation is*

$$\frac{\tau_w}{\rho} = \frac{d}{dx} u_1^2 \theta + u_1 \delta^* \frac{du_1}{dx} \quad (4)$$

*The form of the last term in Eq. (4) anticipates the nature of the experiments to be cited presently. For an incompressible flow with streamwise pressure gradient, but without body forces, there is an energy integral $p + \rho u_1^2/2 = \text{constant}$, or in differential form $\rho u_1 du_1/dx = -dp/dx$. For incompressible flow under gravity force at constant pressure, with g the acceleration of gravity and $g \sin \alpha$ the component in the direction of flow, the corresponding expressions are $\rho u_1^2/2 = \rho g x \sin \alpha + \text{constant}$ and $\rho u_1 du_1/dx = \rho g \sin \alpha$.

where $\tau_w(x)$ is the wall shearing stress, $u_1(x)$ is the velocity of the free stream outside the boundary layer, and $\delta^*(x)$ and $\theta(x)$ are the displacement and momentum thicknesses, defined respectively by

$$\delta^* = \int_0^{\delta} \left(1 - \frac{u}{u_1}\right) dy \quad (5)$$

and

$$\theta = \int_0^{\delta} \frac{u}{u_1} \left(1 - \frac{u}{u_1} \right) dy \quad (6)$$

Experience with Eq. (4) in flows with positive pressure gradient has usually been that the values obtained for τ_w appear to increase rapidly when separation is imminent, contrary to the behavior which might be intuitively expected. In fact, the experiments of Ludwig and Tillmann⁴ were originally designed not to study the law of the wall, but rather to investigate the validity of the momentum-integral equation (4) by providing an independent estimate for τ_w .

It is therefore instructive to compare values of shear obtained by two of the methods already described. In order to avoid differentiation of measured quantities, Eq. (4) may be integrated with respect to x between two stations x_0 and x . Replacing τ_w by ρu_τ^2 , the result of the integration can be expressed by the two equations

$$\Phi(x) = \frac{u_1^2 \theta}{u_0^2 \theta_0} - 1 + \frac{1}{2} \int_{x_0}^x \frac{\delta^*}{\theta_0} d\left(\frac{u_1^2}{u_0^2}\right) \quad (7)$$

and

$$\Phi(x) = \int_{x_0}^x \frac{u_\tau^2}{u_0^2} d\left(\frac{x}{\theta_0}\right) \quad (8)$$

where $u_0 = u_1(x_0)$ and $\theta_0 = \theta(x_0)$.

The dimensionless function $\Phi(x)$ may be evaluated experimentally from Eq. (7) if δ^* , θ , and u_1 are known as functions of x . Quite independently, the same function $\Phi(x)$ may be evaluated from Eq. (8)

if the friction velocity u_τ is obtained by fitting the velocity profile $u(y)$ to the hypothetical law of the wall.

2. Presentation of Data. The discussion will be limited to data obtained at reasonably large Reynolds numbers in experiments at reasonably large scale.* The experimental point of departure is flow

* This survey of experimental data includes certain material which has not previously been reported in detail in the literature. For their courtesy in proving this material I am indebted to F. Clauser of the Johns Hopkins University, Baltimore; Smith J. DeFrance of the N.A.C.A. Ames Aeronautical Laboratory, Moffett Field; W. Tillmann of the Max-Planck-Institut für Strömungsforschung, Göttingen; K. Wieghardt of the Institut für Schiffbau, Hamburg; and A. Kuethe of the University of Michigan, Ann Arbor. I am also indebted to F. Goddard of the Jet Propulsion Laboratory, Pasadena, for making available the services of the JPL computing section.

at constant pressure, for which some mean-velocity measurements of Wieghardt¹⁴ for a free-stream velocity of 33 meters per second are shown in Fig. 2. Here and in the fifteen following figures, the mean-velocity profiles shown are typical of the measurements, although some of the profile data have occasionally been omitted for reasons of economy in the graphical presentation.

All of the profiles, whether shown in the figures or not, have first been individually fitted to the logarithmic region of the law of the wall, i.e. to the formula $u/u_\tau = 5.75 \log_{10} y u_\tau / \nu + 5.10$, and

the resulting values of u_1/μ_T have then been smoothed where necessary. In the fitting operation it has generally been assumed that the measurements for values of $y\mu_T/\nu$ less than about 200 may be unreliable as a result of large fluctuations in velocity, wall interference, poor probe sensitivity at small mean velocities, probe position error, or uncertainty in the static pressure. For consistency, therefore, the contribution to δ^* and Θ of the sublayer and of the logarithmic region have been computed for the function f of Fig. 1 and Ref. 12 rather than for the actual measurements.

Each of Figs. 2 - 17 includes a sketch showing both the geometry of the experiment and the physical extent $\delta(x)$ of the shear flow. Finally, each of Figs. 2 - 17 includes a comparison of the two functions $\Phi(x)$ of Eqs. (7) and (8), represented by open points and by a solid line respectively. Agreement in the slope of the two functions indicates that the flow in question is consistent with the logarithmic law of the wall displayed in Fig. 1.

3. Unseparated Flows. Wieghardt's measurements of boundary-layer growth for a uniform external stream have already been presented in Fig. 2. Wieghardt¹⁵ also investigated the effect of increasing the tunnel turbulence level by means of a coarse screen, obtaining the mean-velocity profiles shown in Fig. 3. Using the same channel and instrumentation, Ludwig and Tillmann⁴ observed a turbulent boundary-layer flow in a negative pressure gradient, with the result shown in Fig. 4. These particular profile measurements, and those of Figs. 11 and 12 below, are the ones originally cited by Ludwig and Tillmann in their cogent paper⁴ on the law of the wall.

Some measurements of flow near the lower boundary of a stream accelerating under the force of gravity at essentially constant pressure have been reported by Bauer¹⁶. The fluid is water traversing the face of a model spillway; data for flow over a smooth plane surface at an angle of 20° , 40° , and 60° with the horizontal are reproduced in Figs. 5, 6, and 7. In each case the body force per unit volume $\rho g \sin \alpha$ is independent of both x and y , and so plays the same role as a constant pressure force per unit volume dp/dx . Except where the nominal boundary-layer thickness exceeds half of the total water depth, values of wall shearing stress obtained from the law of the wall (3) are in excellent agreement with values obtained from the momentum-integral equation (4).

4. Flows Approaching Separation. Extensive measurements in a flow approaching separation have been made by Schubauer and Klebanoff¹⁷ on a large airfoil at the National Bureau of Standards. Typical mean-velocity profiles are shown in Fig. 8. Upstream of the 7-foot station, the surface shearing stress and the free-stream dynamic pressure both increase in the direction of flow. Between $x = 7$ feet and $x = 18$ feet the shear and the pressure are nearly constant. The region of rising pressure begins at $x = 18$ feet, and separation occurs at about $x = 25.7$ feet.

A similar study of a boundary-layer near separation is available in some work of Newman¹⁸ for which the mean-velocity data are presented in Fig. 9. Because Newman measured the static pressure variation within the boundary layer, and also made a plausible correction to his observed mean-velocity profiles for instrumental errors caused

by turbulence, these data are among the most accurate and detailed which are available. Newman, like Schubauer and Klebanoff, also measured turbulence intensities and turbulent shearing stress within the shear flow.

Boundary-layer flow in diffusers of constant width and rectangular section has been studied by Kehl¹⁹, by Ludwig and Tillman⁴, and by Clauser⁵, with the results shown in Figs. 10 through 14. In none of these five experiments did separation actually occur, and in the last two it was deliberately prevented.

5. Flows Following Reattachment. Turbulent boundary-layer flow following reattachment downstream of a separation bubble has been investigated by McCullough and Gault²⁰. Data for the upper surface of an NACA 64A006 airfoil section at an angle of attack of 5° are reproduced in Fig. 15.

Reattachment of separated flow downstream of a tripping device or spoiler, in flow with nominally constant pressure, is illustrated in Figs. 16 and 17 for some measurements of Klebanoff and Diehl⁹ and of Tillmann²¹. In the experiment of Klebanoff and Diehl transition occurred at the spoiler, which was a 1/4-inch diameter rod at the 4-foot station of the plate. In the experiment of Tillmann the boundary layer was turbulent well upstream of the spoiler, which was a rectangular ledge 1.2 cm. square at the 2.02-meter station. In both cases it may be noted that the flow far downstream has apparently not recovered from the effects of the enforced separation, as the mean-velocity profiles do not resemble the profiles for flow at constant pressure shown in Fig. 2.

6. Evaluation. Manifestly, the data cited in the previous section do not provide a test of the hypothetical law of the wall alone, but a joint test of the law of the wall together with the turbulent boundary-layer approximation and the assumption of two-dimensional mean flow.

These data confirm that the momentum-integral equation (4) cannot be relied upon to give accurate values of surface shearing stress in the neighborhood of separation, as the left side of Eq. (4) is then a small difference between two large quantities on the right. Consequently, large errors in τ_w may be encountered either as a result of inconspicuous departures from two-dimensional mean flow or as a result of the omission from the boundary-layer approximation of certain terms involving the Reynolds normal stresses and the pressure variation normal to the wall.

Both Ludwig and Tillmann⁴, using a surface heat-transfer technique, and Schubauer and Klebanoff¹⁷, using extrapolated values of the measured turbulent shear, have found experimentally that the surface shearing stress not only decreases monotonically to zero on approaching a point of separation, but is given accurately in one case, and at least within a constant factor in the other, by the values deduced from the law of the wall. In any event, whether the hypothesis of a universal similarity law is correct for the flows in question or not, it is almost certain from the evidence for example of Figs. 8, 11, and 12 that the momentum-integral equation in the form (4) is seriously in error.

Except for the work of Ludwig and Tillmann, perhaps the most convincing evidence for a universal law of the wall is simply that a distinct logarithmic region occurs in each of several hundred mean-velocity profiles examined here, with very few exceptions; a definite estimate for the wall shearing stress is readily obtained; and this estimate is entirely plausible.

At the same time, it is known¹² that a necessary and sufficient condition for a universal law of the wall, given the boundary conditions of vanishing velocity and Newtonian friction at the surface, is that the ratio u/u_τ is constant on streamlines of the mean flow. The edge of the sublayer, for example, is a mean streamline. This relatively elegant result must surely carry some measure of conviction in any search for a fundamental order and unity in the description of turbulent shear flows.

In view of these remarks, the hypothesis of a universal law of the wall will be accepted for the purposes of the present paper. In fact, it will eventually be suggested that the similarity laws of this and the next section may be concepts sufficiently powerful to allow a quantitative treatment not only of flows approaching or recovering from separation, but of yawed flows and flows which are actually separated from the adjacent wall.

II. THE LAW OF THE WAKE

A. The Momentum Defect Law.

1. Historical Development. The description so far given of the mean-velocity profile in a turbulent shear flow can be summarized by the formula

$$\frac{u}{u_\tau} = f\left(\frac{yu_\tau}{\nu}\right) + h(x, y) \quad (9)$$

where the function h is arbitrary except that it is assumed to be negligibly small in some finite region near the wall, say for y/δ less than about 0.1. By hypothesis, $f(yu_\tau/\nu)$ is a universal function for steady two-dimensional incompressible mean flow near a smooth impermeable plane wall. If the friction is Newtonian at the surface, then $f(yu_\tau/\nu) \rightarrow yu_\tau/\nu$ in the limit $y \rightarrow 0$. Outside the sublayer, on the other hand, f is given by Eq. (3),

$$f\left(\frac{yu_\tau}{\nu}\right) = \frac{1}{\kappa} \ln \frac{yu_\tau}{\nu} + c$$

where $\kappa = 0.40$ and $c = 5.1$.

For uniform pipe and channel flow and for the boundary layer on a flat plate in a uniform stream, Eq. (9) is found experimentally to have the special form

$$\frac{u}{u_\tau} = f\left(\frac{yu_\tau}{\nu}\right) + g\left(\pi, \frac{y}{\delta}\right) \quad (10)$$

where π is a parameter which is independent of x and y . That the

boundary-layer flow in particular has this property is demonstrated by Wieghardt's measurements in Fig. 2.

Profile similarity in terms of the argument y/δ is usually expressed by a relationship known as the velocity-defect law, or more properly the momentum-defect law. Outside the sublayer, it follows from the logarithmic variation of f that

$$\frac{u_1 - u}{u_\tau} = F\left(\pi, \frac{y}{\delta}\right) \quad (11)$$

where $u = u_1$ at $y = \delta$ and, from Eq. (10),

$$F\left(\pi, \frac{y}{\delta}\right) = g(\pi, 1) - g\left(\pi, \frac{y}{\delta}\right) - \frac{1}{\kappa} \ln \frac{y}{\delta}$$

A special form of the relationship (11) was proposed by Darcy nearly a hundred years ago, and again by Stanton in 1911, to describe the mean-velocity profile in turbulent pipe flow. The defect law in the general form (11) was formulated independently in 1932 by von Kármán³, who derived an approximate friction law involving two empirical constants for the turbulent boundary layer with constant pressure. According to experimental evidence from many sources, the defect function $F\left(\pi, \frac{y}{\delta}\right)$ in a given flow is insensitive to roughness at the wall provided that the origin for the normal coordinate y is properly chosen. On the other hand, it appears from a comparison of Figs. 2 and 3 that there is a small dependence of the defect law on the turbulence level in the external stream.

The awkward problem of defining a boundary-layer thickness δ is

usually avoided by observing that δ is proportional* to $\delta^* u_1 / u_\tau$ for

The notation $\delta^ u_1 / u_\tau = \Delta$ has been used by F. Clauser⁵.

any flow with a defect law. For if the displacement thickness δ^* is computed from Eq. (5) for the profile (11), neglecting the departure of the flow in the sublayer from the logarithmic law, there is obtained

$$\frac{\delta^* u_1}{\delta u_\tau} = \int_0^1 F\left(\pi, \frac{y}{\delta}\right) d\frac{y}{\delta} = C(\pi)$$

The particular combination $\delta^* u_1 / \delta u_\tau$ will occupy an important place in the present study. Moreover, the present implicit notation for the parameter π will be replaced in the next section by an explicit formula

$$\pi = \kappa C(\pi) - 1 = \kappa \frac{\delta^* u_1}{\delta u_\tau} - 1$$

2. The Equilibrium Boundary Layer. A brilliant new concept in the experimental definition of turbulent shear flows was recently introduced by F. Clauser⁵, who generalized the idea of a defect law by constructing two boundary-layer flows with positive pressure gradient such that Eqs. (10) and (11) remained valid. The flows in question have already been described in Figs. 13 and 14. Clauser used the term "equilibrium flow" to denote a member of the one-parameter class of flows for which, in the notation of Eqs. (10) and (11), the parameter π is constant.

Examination of Figs. 5, 6, and 7 suggests that the three spillway flows studied by Bauer may be equilibrium flows in the sense of Clauser's definition. So, at least approximately, is the flow with falling pressure studied by Ludwig and Tillmann and reported in Fig. 4.

A comparison of the velocity defect function F for three equilibrium flows can be found in Fig. 18 of Clauser's paper, and is repeated here as Fig. 18. This figure, unfortunately, sheds little light on the way in which the argument y/δ and the parameter π are involved in the function $F(\pi, \frac{y}{\delta})$ of Eq. (11), and therefore does not immediately suggest any useful generalization of the defect law to non-equilibrium flows.

3. The Logarithmic Region. At this point an important further consequence of the defect law in equilibrium flow should be mentioned. In the first instance, the mixing analogy of Prandtl and von Kármán implies a logarithmic variation of the function $f(yu_\tau/\nu)$ in flows for which τ does not depend on y . However, if the law of the wall is universally valid, then the velocity distribution $u(y)$ can be expressed independently of the shear distribution $\tau(y)$, and the arguments of the mixing analogy in favor of a logarithmic mean-velocity distribution are seriously crippled.

It is therefore instructive to consider another argument, first proposed by Millikan²² and based on the wall and defect laws, which also leads to a logarithmic function f in Eq. (2). From the law of the wall, $u/u_\tau = f(yu_\tau/\nu)$, it follows that

$$\frac{y}{u_\tau} \frac{\partial u}{\partial y} = \frac{yu_\tau}{\nu} f' \left(\frac{yu_\tau}{\nu} \right)$$

From the defect law, $(u_i - u)/u_\tau = F(\pi, y/\delta)$, the corresponding expression is

$$\frac{y}{u_\tau} \frac{\partial u}{\partial y} = - \frac{y}{\delta} F' \left(\frac{y}{\delta} \right)$$

where the constant parameter Π has been suppressed for an equilibrium flow. Now suppose that there is a finite region in which the wall and defect laws are simultaneously valid. In this region, the last two equations require

$$\frac{y u_\tau}{\nu} f' \left(\frac{y u_\tau}{\nu} \right) = - \frac{y}{\delta} F' \left(\frac{y}{\delta} \right) = \frac{y}{u_\tau} \frac{\partial u}{\partial y} = \frac{1}{\kappa(x, y)}$$

say. Obviously, $\kappa(x, y)$ is fixed when either of the two variables $y u_\tau / \nu$ or y / δ is specified. But these variables are formally independent of each other, since their ratio $\delta u_\tau / \nu$ may be chosen arbitrarily. It follows that κ must be a constant. Furthermore, on integrating the expression for $\partial u / \partial y$ in the region in question, it is found that

$$f \left(\frac{y u_\tau}{\nu} \right) = \frac{1}{\kappa} \ln \frac{y u_\tau}{\nu} + \text{CONSTANT}$$

in agreement with Eq. (3).

The question naturally arises as to whether or not the inverse of Millikan's problem can be solved. That is, given a universal law of the wall which is logarithmic outside the sublayer, what further assumptions about the motion are necessary in order to establish a defect law? The real purpose of the present paper up to this point has been to prepare the way for the formulation of this question. The purpose of the remaining sections is to present and to exploit one possible answer.

B. The Wake Hypothesis.

1. The Wake Function. It should first be noted that the defect law (11) has at least a limited physical interpretation, in that the loss of momentum is expressed independently of the viscosity. This property, being consistent with the idea of a turbulent rather than a viscous transport process, can reasonably be assumed as in Millikan's argument to apply everywhere outside the sublayer. Furthermore, the observed sensitivity of the momentum defect to external turbulence level and the observed insensitivity to wall roughness are not surprising.

On the other hand, the various mean-velocity profiles so far studied are quite systematic in coordinates $(u/u_\tau, y u_\tau/\nu)$ which involve the viscosity of the fluid. In fact, once the universal law of the wall is accepted, it is difficult to escape the conviction that an arbitrarily chosen profile is completely determined when the free-stream point $(u_1/u_\tau, \delta u_\tau/\nu)$ is specified. To illustrate this remark, Fig. 19 shows several mean-velocity profiles selected from various boundary-layer flows described earlier*. These profiles have essentially the

* Reading from left to right, the profiles are taken from Fig. 16 (Klebanoff and Diehl, Ref. 9, Sta. 4.25), Fig. 14 (Clauser, Ref. 5, Series 2, Sta. 108), Fig. 9 (Newman, Ref. 18, Sta. D and C), Fig. 14 (Clauser, Ref. 5, Series 2, Sta. 230), and Fig. 12 (Ludwig and Tillmann, Ref. 4, Channel VIb, Sta. 3.73 and 3.53).

same defect law, which is to say the same value of the parameter Π according to Eq. (10), in spite of wide variations in environment.

Taking these properties together, it is something of an anti-climax to discover that the puzzle of the defect law is apparently a simple one. The key lies not in a study of the defect function F of Eq. (11), but in a study of the original function $g(\pi, \frac{y}{\delta})$ of Eq. (10), which gives the departure of the mean-velocity profile from the logarithmic law of the wall. For the three equilibrium flows of Fig. 18, this departure is shown in Fig. 20, using a linear scale for y/δ . There is a striking resemblance between the three curves, including a characteristic anti-symmetry about a midpoint. But this resemblance is obviously not confined to equilibrium flows if, as has just been suggested in Fig. 19, an arbitrary profile in non-equilibrium flow coincides in the coordinate system $(u/u_\tau, y u_\tau/\nu)$ with a profile from some member of the one-parameter family of equilibrium flows.

In view of these remarks, and especially in view of Fig. 20, the mean-velocity profile may tentatively be written in the form

$$\frac{u}{u_\tau} = f\left(\frac{y u_\tau}{\nu}\right) + \frac{\pi(x)}{\kappa} w\left(\frac{y}{\delta}\right) \quad (12)$$

where $\pi(x)$ is a profile parameter, as before, but the function $w(y/\delta)$ is now supposedly common to all two-dimensional incompressible turbulent boundary-layer flows*.

*The combination $\pi(x)w(y/\delta)$ in Eq. (12) should be compared with the function $g(\pi, y/\delta)$ in Eq. (10). If π does not depend on x , then both g and πw are functions of y/δ only. This is the property assigned to equilibrium flows by Clauser. The present formulation of the mean-velocity profile is however more

general than Eq. (10), in the sense that the law of the wake, although a restricted form of Eq. (10) which is itself a special form of Eq. (9), is here assumed to apply for non-equilibrium flows.

The introduction of a second universal function in the mean-velocity profile will be referred to as the wake hypothesis, for reasons which will become apparent, and the function $w(y/\delta)$ in Eq. (12) will be referred to as the law of the wake.

2. Normalizing Conditions. In order to test the hypothesis of a universal wake function in Eq. (12), it is necessary first to define the thickness δ and to specify some normalizing factor for w . To this end, the displacement thickness δ^* may be computed from the definition, Eq. (5), for the particular profile given by Eq. (12). Neglecting the departure of the flow in the sublayer from the logarithmic wall law, there is obtained

$$\delta^* = \delta \frac{u_\tau}{u_i} \left(\frac{1}{\kappa} + \frac{\pi}{\kappa} \int_0^{w_i} \frac{y}{\delta} dw \right)$$

where w_i is tentatively defined as the maximum value of w . It is therefore convenient to take as a first normalizing condition

$$\int_0^{w_i} \frac{y}{\delta} dw = 1 \quad *$$
(13)

A second normalizing condition is suggested by the nearly anti-symmetric form of the curves in Fig. 20. The maximum value of w will occur very nearly at $y/\delta = 1$ provided that

$$w(1) = w_1 = 2 \quad (14)$$

Now $w(y/\delta)$ is by hypothesis a universal function, so that the boundary-layer thickness δ is uniquely defined in terms of δ^* by the integral condition (13) and the maximum condition (14). That is, the two relationships

$$\frac{u_1}{u_\tau} = \frac{1}{\kappa} \ln \frac{\delta u_\tau}{\nu} + c + \frac{2\pi}{\kappa} \quad (15)$$

and

$$\kappa \frac{\delta^* u_1}{\delta u_\tau} = 1 + \pi \quad (16)$$

together with the identity

$$\left(\frac{\delta^*}{\delta} \right) \left(\frac{u_1}{u_\tau} \right) = \left(\frac{\delta^* u_1}{\nu} \right) / \left(\frac{\delta u_\tau}{\nu} \right)$$

are sufficient to determine all five of the dimensionless parameters u_1/u_τ , δ^*/δ , $\delta u_\tau/\nu$, $\delta^* u_1/\nu$, and π (or $\delta^* u_1/\delta u_\tau$) when any two are given*. For example, if the two known quantities are u_1/u_τ

* Given the two supposedly universal functions $f(yu_\tau/\nu)$ and $w(y/\delta)$ in Eq. (12), it is clear that the dimensionless mean-velocity profile including the sublayer flow is completely determined by any two of these five parameters. A great variety of two-parameter functional relationships, e.g.

$u/u_1 = \varphi(y/\delta, \delta^*u_1/\nu, \pi)$, is therefore implied by, and can be explicitly obtained from, the original Eq. (12) for the mean-velocity profile in a turbulent boundary layer.

and δ^*u_1/ν , as is supposedly the case for the data cited earlier in this study, then Eqs. (15) and (16) lead to a simple transcendental equation for π ;

$$2\pi - \ln(1 + \pi) = \kappa \frac{u_1}{u_\tau} - \ln \frac{\delta^*u_1}{\nu} - \kappa c + \ln \frac{1}{\kappa} \quad (17)$$

3. Profile at Separation. Eq. (12) as originally written is not in a convenient form for use near a point of separation or reattachment. However, on multiplying by u_τ/u_1 and using Eq. (16) to eliminate π , there is obtained

$$\frac{u}{u_1} = \frac{u_\tau}{u_1} f\left(\frac{y u_\tau}{\nu}\right) + \left(\frac{\delta^*}{\delta} - \frac{1}{\kappa} \frac{u_\tau}{u_1}\right) w\left(\frac{y}{\delta}\right)$$

If u_τ is put equal to zero in this expression, the result is evidently

$$\frac{u}{u_1} = \frac{\delta^*}{\delta} w\left(\frac{y}{\delta}\right) = \frac{1}{2} w\left(\frac{y}{\delta}\right)$$

which does not involve either ν or κ . It follows, again since $w(y/\delta)$ is by hypothesis a universal function, that the flow at a point of separation or reattachment is a pure wake flow, with u_1 as characteristic velocity and δ as characteristic length. Moreover,

certain numerical values can be assigned in advance to the ratios δ^*/δ , θ/δ , and δ^*/θ .

The definition of δ adopted here takes account of the nearly antisymmetric variation of w by requiring $\delta^*/\delta = \frac{1}{2}$ at separation. A corollary result, anticipating numerical values of the next section, is $\theta/\delta = 0.12$ approximately. On the other hand, the prediction $\delta^*/\theta = 4.2$ approximately at separation or reattachment is a result which is relatively free of preconceptions about the form of the function w . It should be noted that this prediction, although not incompatible with the experience of von Doenhoff and Tetervin²³ and others, is based on examination of the mean-velocity profile in flows which need not be close to separation. It may also be noted that the present formulation also requires the profile parameter of Gruschwitz²⁴, $\eta = 1 - u^2(\theta)/u^2(\delta)$, to have a fixed value at separation.

4. Test of the Hypothesis. For obvious reasons, the existence and form of the hypothetical wake function $w(y/\delta)$ are most readily investigated in flows with a large wake component. Fig. 20 shows, with the normalizing conditions (13) and (14), the wake function w for several mean-velocity profiles taken from the present survey. At least for unseparated flows the wake hypothesis appears to be a useful concept, and a tentative determination of the wake function $w(y/\delta)$ is therefore tabulated in Table I and plotted in Figs. 19 and 20.

A few exceptions to the law of the wake can be found among the numerous profiles presented earlier. For example, it does not appear to be possible to find parameters u_T , δ , and Π in the

general formula (12) such that the most westerly profile in Fig. 19 can be represented within the apparent experimental accuracy. However, this profile was obtained about two boundary-layer thicknesses downstream of reattachment, and there is some uncertainty about the static pressure within the shear flow. Occasionally, for example in fitting the data of Schubauer and Klebanoff, as shown in Fig. 21, slight revisions have been made in the original values of u_1/u_T , δ , and π obtained from consideration of the law of the wall alone.

It appears that the two-component profile equation (12) allows a quite satisfactory fit for the data of Newman, as shown in Fig. 22; of Kehl; of Clauser; of Ludwig and Tillmann; of McCullough and Gault at 5° angle of attack, as shown in Fig. 23; and of Tillmann for reattaching flow, as shown in Fig. 24.

Finally, it may be remarked that Wieghardt's experiments in Fig. 3 show a definite change in shape as well as in amplitude for the wake component in flow at constant pressure when the free-stream turbulence level is increased. The term "universal function" applied to the law of the wake therefore implies that the external turbulence level is low, much as the same term applied to the law of the wall implies negligible surface roughness.

III. APPLICATIONS

A. The Equations of Mean Motion .

1. The Turbulent Shearing-Stress Profile. To the extent that the similarity laws of the two preceding sections are not founded on unambiguous physical principles^{*}, these laws are not theoretical laws

^{*} A tentative and incomplete physical equivalent for the law of the wall is discussed in Ref. 12.

in the usual sense. That is, they cannot at present be generalized with confidence to conditions outside the range of observation. At the same time, these similarity laws go well beyond the usual limits of dimensional analysis. In particular, they can be combined with the equations of motion to take advantage of the fact that a complete analytical description of the mean-velocity field implies complete analytical knowledge both of the streamline pattern and of the shear field, at least within the usual boundary-layer approximation.

For example, the continuity equation

$$v = - \int_0^y \frac{\partial u}{\partial x} dy \quad (18)$$

may first be satisfied by introducing a stream function $\psi(x,y)$ such that $u = \partial\psi/\partial y$ and $v = -\partial\psi/\partial x$; ψ is then constant on streamlines of the mean flow. But Eq. (12), neglecting the departure of the profile in the sublayer from the logarithmic law of the wall, requires

$$\frac{\psi}{v} = \frac{1}{v} \int_0^y u dy = \frac{y u_\tau}{v} \left(\frac{u}{u_\tau} - \frac{1}{\kappa} \right) - \frac{\pi}{\kappa} \frac{\delta u_\tau}{v} \int_0^w \frac{y}{\delta} dw \quad (19)$$

A formula for the normal component of velocity may be obtained from $v = -\partial\psi/\partial x$, using Eq. (19) for $\psi(x, y)$, or directly from the continuity equation (18), using Eq. (12) for $u(x, y)$. In either case it is found that

$$\frac{v}{u} = -\frac{y}{u_\tau} \frac{du_\tau}{dx} - \frac{yu_\tau}{\kappa} \frac{w}{u} \frac{d\pi}{dx} + \frac{1}{\kappa u} \frac{d\pi}{dx} \frac{du_\tau}{dx} \int_0^w \frac{y}{\delta} dw \quad (20)$$

This expression is an exact consequence of Eq. (12), in the sublayer as elsewhere. Its application in the calculation of the shear profile is most easily shown by putting $-\partial v/\partial y$ for $\partial u/\partial x$ in the boundary-layer momentum equation

$$\tau = \tau_w - y\rho u_1 \frac{du_1}{dx} + \rho \int_0^y \left(u \frac{\partial u}{\partial x} + v \frac{\partial u}{\partial y} \right) dy \quad (21)$$

to obtain

$$\frac{\tau}{\tau_w} = 1 - \frac{yu_1}{u_\tau^2} \frac{du_1}{dx} - \int_0^{v/u} \left(\frac{u}{u_\tau} \right)^2 d\left(\frac{v}{u} \right) \quad (22)$$

2. Flow at Constant Pressure. For flow at constant pressure, i.e. for π and u_1 constant, the expressions (18) and (22) may be evaluated explicitly for the profile given by Eq. (12). The result can be written in the form*

*The quantity in brackets in Eq. (24) is subject to the usual approximation in the sublayer, whereby for example $\int f dz$ is written $\int z - \int z df$ and df is replaced by $dz/\kappa z$ as if the function f were logarithmic everywhere.

$$\frac{v}{u} = - \frac{y}{u_T} \frac{du_T}{dx} \left[1 + \frac{u_1}{u} (\omega_1 - 1) \right] \quad (23)$$

and

$$\begin{aligned} \kappa^2 \left(1 - \frac{\tau}{\tau_w} \right) = & - \frac{y}{u_T} \frac{du_T}{dx} \left[\left(\kappa \frac{u}{u_T} \right)^2 - 2 \left(\kappa \frac{u}{u_T} \right) \omega_1 \right. \\ & \left. + \left(\kappa \frac{u}{u_T} \right) \left(\kappa \frac{u_1}{u_T} \right) (\omega_1 - 1) - 2 \left(\kappa \frac{u_1}{u_T} \right) (\omega_2 - \omega_1) + 2 \omega_2 \right] \quad (24) \end{aligned}$$

where ω_1 and ω_2 are auxiliary functions which depend on an argument $\xi = y/\delta$ and a parameter π ,

$$\omega_1(\pi, \xi) = 1 + \frac{\pi}{\xi} \int_0^{w(\xi)} \xi' dw' \quad (25)$$

$$\omega_2(\pi, \xi) = \omega_1 + \frac{\pi}{\xi} \int_0^{w(\xi)} \xi' \ln \frac{\xi}{\xi'} dw' + \frac{\pi^2}{\xi} \int_0^{w(\xi)} \xi' (w - w') dw' \quad (26)$$

and $w(\xi)$ is the wake function. The quantities $\omega_1(\pi, \xi)$ and $\omega_2(\pi, \xi)$ are tabulated together with w in Table I.

Finally, the derivative du_T/dx in Eq. (24) may be disposed of by putting $y = \delta$ to obtain*

$$\kappa^2 = - \frac{\delta}{u_T} \frac{du_T}{dx} \left[\left(\kappa \frac{u_1}{u_T} \right)^2 \Omega_1 - 2 \left(\kappa \frac{u_1}{u_T} \right) \Omega_2 + 2 \Omega_2 \right] \quad (27)$$

* This expression, like Eq. (37) of Ref. 10, is a special form of the momentum-integral equation (4), and may be used to define a length Reynolds number. The present definition of the

thickness δ , however, requires the numerical constants $\varphi(1) = 7.90$, $C_1 = 4.05$, and $C_2 = 29.0$ of Ref. 10 to be replaced, anticipating the value $\Pi = 0.55$, by $C + 2\Pi/\kappa = 7.85$, $\Omega_1/\kappa = 3.88$, and $2\Omega_2/\kappa^2 = 26.4$.

with $\Omega_1(\Pi) = \omega_1(\Pi, 1) = 1 + \Pi$ and $\Omega_2(\Pi) = \omega_2(\Pi, 1) = 1 + 1.600\Pi + 0.761\Pi^2$.

Klebanoff⁸ has recently measured the turbulent shearing-stress distribution in a boundary layer with constant pressure such that

$$\begin{aligned}\delta^* u_1 / \nu &= 9,700 \\ \delta^* &= 0.400 \text{ inches}\end{aligned}$$

The experimental mean-velocity profile for this flow has already been shown in Fig. 1. However, in order to make the present calculation independent of Klebanoff's measurements, it is convenient to estimate the parameter Π from the data of Wiegardt in Fig. 2. Using either Eq. (12) and the observed maximum excursion from the logarithmic law, or Eq. (17) and the experimental values for u_1/μ_T and $\delta^* u_1/\nu$, it is found that Π is very nearly 0.55 for flow at constant pressure. Then from Eqs. (15) and (16), with $\delta^* u_1/\nu = 9,700$ and $\Pi = 0.55$,

$$\delta u_T / \nu = 2,500$$

$$u_1 / \mu_T = 27.4$$

$$\delta^* / \delta = 0.142$$

Furthermore, with $\delta^* = 0.400$ inches

$$\delta = 2.83 \text{ inches}$$

The profile u/u_T computed as a function of $y u_T/\nu = (y/\delta) \delta u_T/\nu$ from Eq. (12) is plotted in Fig. 1. The excellent agreement with Klebanoff's measurements is to be expected, in view of the efforts made at the National Bureau of Standards⁹ to insure that the flow in question would be typical of the fully-developed boundary layer.

The profile $\tau/q = (\tau/\tau_w)(2u_T^2/u_i^2) = -2\overline{u'v'}/u_i^2$ computed from Eqs. (24) and (27) is plotted against y/δ in Fig. 25, together with measured data using the revised value for δ of 2.83 inches. The agreement here between measured and computed shear supports a finding of Liepmann and L  ufer²⁵, in that the phenomenon of intermittency apparently does not invalidate either the conceptual or the experimental procedure for defining mean velocity and mean turbulent shear.

Finally, to establish the extent of the region of intermittent turbulence in terms of the coordinate y/δ occurring in the law of the wake, Fig. 25 also shows Klebanoff's measurements of the intermittency factor γ , defined as the fraction of the time that the flow is turbulent. The mean position of the turbulent boundary, i.e. the point $\gamma = 1/2$, is found to be at $y/\delta = 0.825$, with a standard deviation of 0.148 about the mean.

3. Flow Approaching Separation. Schubauer and Klebanoff¹⁷ and Newman¹⁸ have recently carried out hot-wire measurements of turbulent shear in flows approaching separation. The representation of the mean-velocity field by the general profile equation (12) has already been illustrated in Figs. 21 and 22 for the flows in question. The corresponding shear profiles, computed from Eqs. (20) and (22), are shown in the same figures together with the profiles determined experimentally. The values of $\overline{u'v'}$ reported by Schubauer and Klebanoff have been

reduced by 31 percent in view of the excessively large values obtained for τ_w when $\tau(y)$ is extrapolated to $y = 0$. It is likely that the hot-wire data are in fact too high, most probably as a result of over-compensation.

Unfortunately, these shear calculations can be attempted only for regions in which the mean-velocity field is in reasonable agreement with the momentum-integral condition expressed by Eq. (4). Elsewhere in the flow it is found to be possible to satisfy only one of the two boundary conditions (1) $\tau = 0$ at $y = \delta$ or (2) $\tau = \rho u_T^2$ at $y = 0$, u_T being derived from a fit to the law of the wall. The alternative calculations are shown in Figs. 21 and 22 by the dashed lines. Because Eq. (22) is precisely equivalent to Eq. (4), the values obtained for τ_w on requiring $\tau = 0$ at $y = \delta$ are the same as the values implied by the slope of the function $\Phi(x)$ defined by Eq. (7) and plotted in Figs. 8 and 9 for the data of Schubauer and Klebanoff and of Newman respectively. The discrepancies encountered in τ_w are probably too large to be caused entirely by neglect in Eq. (22) of the Reynolds normal stresses and the pressure variation $\partial p / \partial y$, although this question is still open.

Another explanation for the failure of the two-dimensional momentum-integral equation (4) has been suggested on experimental grounds by Tillmann²⁶, Clauser⁵, and others. The displacement of fluid is assumed to be described by the streamline slope v/u , obtained by integrating the continuity equation $\partial u / \partial x + \partial v / \partial y = 0$. This displacement will be affected by lateral convergence or divergence of the general flow if $\partial w / \partial z \neq 0$. There may be an additional lateral component of displacement in strongly wake-like flows if the pressure gradient is not in the

same direction as the external flow^{*}. At the same time it does not

^{*} See Section III, Part B-2, on yawed and separated flows.

follow that an accurate estimate of the wall shearing stress is not provided by the two-dimensional law of the wall. Moreover, difficulties with lateral flow would not necessarily be revealed by a study of the mean-velocity profile $u(y)$ measured at various lateral stations.

If τ_w is known but the values taken for v/u are even slightly in error, the right-hand side of Eq. (22) will not vanish at the outer edge of the boundary layer. Conversely, large errors in τ_w may be encountered on requiring $\tau = 0$ at $y = \delta$. At one station in each of Figs. 21 and 22 the quantities

$$1 - \frac{y u_1}{u_\tau^2} \frac{du_1}{dx}$$

and

$$- \int_0^{v/u} \left(\frac{u}{u_\tau} \right)^2 d \left(\frac{v}{u} \right)$$

are plotted separately in order to illustrate the extreme sensitivity of their sum τ/τ_w to small variations in v/u or in du_1/dx . As a tentative correction for three-dimensional flow, finally, the streamline slopes v/u have been multiplied by suitable constant factors close to unity in order to satisfy both boundary conditions on τ . The corrected shear profiles are shown by the solid lines in Figs. 21 and 22.

B. Other Applications.

1. Physical Interpretation. In this paper the term "wake flow" has consistently been used to denote the function $w(y/\delta)$ in Eq. (12). The reason for this choice of terminology can be found in some measurements by Liepmann and Laufer²⁵ in a plane half-wake or half-jet; that is, in the wedge-shaped region of turbulent mixing between a uniform flow and a fluid at rest.

The dimensionless mean-velocity profiles for the fully-developed half-wake were originally reported by Liepmann and Laufer to satisfy a similarity law corresponding to a linear growth of the shear flow. These same profiles, after a further translation and change of scale for the coordinates*, are compared in Fig. 20 with the wake function w

* The present variable $\zeta = y/\delta$ is related to the original variable $\sigma y/x$ in Fig. 13 of Ref. 25 by the expression $\zeta = 0.505 + 0.331 \sigma y/x$. When $\zeta = 0$, $\sigma y/x = -1.52$; when $\zeta = 1$, $\sigma y/x = 1.50$. Then $\sigma \delta/x = 3.02$ and it follows if $\sigma = 12$ that $\delta/x = 0.252$ radians or 14.4 degrees.

for flow in a boundary layer. The residual velocity near $y/\delta = 0$ in the figure is the normal component of velocity associated with fluid entrainment, and agrees in magnitude with the value $v/u_1 = 0.03$ implied at $y/\delta = 0$ by the equations of mean motion for the half-wake.

Although the motion represented by the upper curve in Fig. 21 is bounded on the low-velocity side by fluid at rest, rather than by a solid wall, there can be little doubt that the similarity between the various experimental curves in the figure is more than accidental, and that substantially the same physical phenomenon is involved. This obser-

vation suggests a useful interpretation of flow in a boundary layer, an interpretation illustrated in Fig. 26 for a flow which is proceeding from separation to separation through a region of attached flow. The dashed lines in the figure show the wake-like structure represented by the function $w(y/\delta)$. The associated velocity defect $u_\tau - u$ is given by $\pi u_\tau (2 - w)/\kappa$, and the intercept at $y = 0$ of the equivalent wake profile differs from the velocity in the free stream by an amount $2\pi u_\tau/\kappa$.^{*} The latter quantity is therefore a better measure of the strength of the wake component than π itself.

When the flow is bounded by a wall, it is ultimately necessary to satisfy the boundary conditions of vanishing velocity and Newtonian friction at the surface. These conditions impose a further constraint on the flow whose effect is to modify the mean-velocity distribution, as shown by the solid lines in Fig. 26. Near the wall, where the wake mean velocity is nearly constant, the constraint manifests itself in damping of the fluctuations and in the similarity relationship known as the law of the wall. It is important to note, however, that the wall constraint penetrates the entire boundary layer, inasmuch as a logarithmic increment in the mean-velocity profile may always be identified when u_τ is different from zero.

It is admittedly an oversimplification, although perhaps a useful one, to suppose that the wake component ought to be viewed as a large-scale mixing process constrained primarily by inertia, with δ as characteristic scale, while the wall component is viewed as a small-scale mixing process constrained primarily by viscosity, with ν/u_τ as characteristic scale. If the streamwise mean-velocity distribution in a turbulent boundary layer can in fact be expressed as a linear combi-

nation of wall and wake components, as in Eq. (12), then so can the displacement thickness δ^* , the normal mean-velocity component v , and the mean stream function ψ , all of which are obtained from $u(x, y)$ by linear operations. Not so, however, for the flow inclination v/u , the momentum thickness θ , or the shearing stress τ , and most emphatically not so for the turbulent fluctuations except insofar as the wake and wall components might be expected to contribute more strongly to the small and large wave-number regions of the spectrum respectively. On the other hand, a foundation has been laid in the present paper for the comparison, at corresponding points in various free and bound shear layers, of measurements of intermittency factor as well as of spectra and intensity of various fluctuating quantities.

Finally, in the event that the parameter Π is constant in a turbulent boundary layer, a certain balance is implied between the constraints imposed by inertia and by viscosity and between the two mixing processes. This balance is quite precisely measured in Eq. (16) by the magnitude of the parameter Π or alternatively of the combination $\delta u_1^* / \delta u_\tau$. From the point of view adopted in these paragraphs, therefore, Clauser's choice of the term "equilibrium flow" to describe the situation when Π is constant may well be regarded as inspired.

It should be noted that Lees and Crocco²⁷ have recently attempted a qualitative analysis of turbulent shear flows in which they visualize a continuous spectrum of mixing processes having both wake-like and boundary-layer-like properties. The concept of two flow components, one depending on friction and the other on the cumulative effect of pres-

sure gradient, has also been independently advanced by Ross and Robertson²⁸ and by Rotta²⁹, both of whom used a term linear in y to represent what is called here the wake function $w(y/\delta)$. These authors did not give any interpretation for either of the mean-velocity functions and were therefore able to recommend their formulation of the problem only as a useful engineering approach, although Rotta obtained relationships which anticipate the present work. As a matter of historical interest, it should also be noted that a much earlier attempt by Millikan²² to examine the function denoted by $h(x, y)$ in Eq. (9) was unsuccessful because the experimental data studied were not sufficiently precise. These efforts have certainly contributed, if not to the specific concept called the law of the wake, at least to the atmosphere in which this concept was evolved.

2. Yawed and Separated Flows. The present formulation of the mean-velocity profile in Eq. (12) automatically distinguishes between wake-like flows, for which Π is positive, and jet-like flows, for which Π is negative. The turbulent boundary layer can ordinarily be expected to have a wake-like profile, as illustrated in Fig. 26. However, examples of jet-like flows may be found in some measurements by Kehl¹⁹ in a doubly-converging channel, and possibly in some data obtained by Korkegi³⁰ in an adiabatic compressible boundary layer at constant pressure at a Mach number of 5.8. These examples lie outside the scope of the present discussion, which is not concerned specifically with three-dimensional or compressible flows. It may be noted, however, that if the mean velocity u within the boundary layer is not to exceed the free-stream velocity u_∞ , in a

fluid of constant density, then $\partial u / \partial y$ from Eq. (12) must be positive. This is to say that $-\pi \xi dw/d\xi$, where $\xi = y/\delta$, should be less than unity. Table I then leads to the estimate $\pi > -0.52$ approximately. On the other hand, if the density is not constant, the question of interpretation of the parameter π must obviously yield to the prior question of the effect of density changes on the equation (12) describing the mean-velocity profile.

For a given fluid, Eq. (12) and Table I of the present paper and Table I of Ref. 12 allow the velocity field, including the flow in the sublayer, to be constructed whenever three of the four parameters u_1 , u_τ , δ , and π are given. The fourth of these quantities is determined by Eq. (15),

$$\kappa \frac{u_1}{u_\tau} = \ln \frac{\delta u_\tau}{\nu} + \kappa c + 2\pi$$

Once a sign convention is adopted for u_τ , a corresponding construction can obviously be carried out for flows which are actually separated from the adjacent surface, as has in fact been done at one station in Fig. 23. Even this generalization may be unnecessarily restrictive, if it is eventually found that yawed or three-dimensional flows can be usefully represented by taking the wall and wake components of the profile as vector rather than scalar functions of position. Explicitly, suppose that Eq. (12) is rewritten in the form

$$\vec{q} = \vec{q}_f + \vec{q}_w \quad (28)$$

where

$$\vec{g}_f = \vec{g}_\tau f\left(\frac{y g_\tau}{\nu}\right) \quad (29)$$

and

$$\vec{g}_w = \frac{\pi \vec{g}_\tau}{\kappa} w\left(\frac{y}{\delta}\right) \quad (30)$$

In these expressions $f(y g_\tau / \nu)$ and $w(y / \delta)$ are identified with the scalar functions previously described for two-dimensional flow, and g_τ is defined as the magnitude of a friction-velocity vector \vec{g}_τ taken parallel to the surface shearing stress $\vec{\tau}_w$,

$$\vec{\tau}_w = \rho g_\tau \vec{g}_\tau \quad (31)$$

Furthermore, both \vec{g}_τ and π are assumed to depend on two space coordinates, say x and z . Then the parameter $\pi(x, z)$, if \vec{g}_f and \vec{g}_w are not parallel vectors, should presumably be interpreted as a tensor; i. e. as a linear operator having the properties of a square matrix. It also follows that the generalized vector friction law is

$$\vec{g}_f = \vec{g}_\tau f\left(\frac{\delta g_\tau}{\nu}\right) + \frac{2 \pi \vec{g}_\tau}{\kappa} \quad (32)$$

This notation is highly tentative, and may have to be revised after more data on yawed flows become available. In particular, the definition (31) for g_τ is not perfectly consistent with the streamline hypothesis of Ref. 12 if $\vec{\tau}_w$ is an arbitrary continuous function of two

coordinates on the surface. However, the notation does allow the interpretation already proposed, that the flow near the surface where the wake component is small should have the same direction and sense as the surface shearing stress. Thus the concept of a constraint provided by friction is a vector concept.

Given a mean-velocity profile in yawed flow, the vector nature of the wall and wake components can be tested in five steps. First, the direction of the mean flow near the surface, which is also by assumption the direction of the shearing-stress vector $\vec{\tau}_w$ and of the wall component \vec{q}_f , is noted. Second, the component of mean velocity in this direction is plotted in coordinates $(\vec{q} \cdot \vec{q}_\tau / q_\tau^2, \gamma q_\tau / \nu)$ appropriate to the law of the wall; a fit to the function f then yields a value for q_τ . Third, the thickness δ is estimated from this same plot, for example as twice the value of γ for which the profile reaches half of its maximum excursion from the law of the wall. Fourth, the "wall" vector $\vec{q}_{f1} = \vec{q}_\tau f(\delta q_\tau / \nu)$ is computed and subtracted from the free-stream vector \vec{q}_f to obtain the "wake" vector $\vec{q}_w = 2\pi \vec{q}_\tau / \kappa$. Finally, the profile is resolved in oblique coordinates determined by the direction of the wall and wake vectors.

Remarkably few studies of yawed or separated turbulent flows have been reported in the experimental literature, in spite of the practical importance of such flows. An examination of the data of Gruschwitz³¹ in a curved channel suggests that serious errors were introduced in the mean-velocity measurements near the surface by the use of a periscope probe. In particular, the profiles in the straight portion of the channel differ from the consensus of data obtained by

other investigators under similar conditions. Fortunately the hot-wire measurements of Kuethe, McKee, and Curry³² on a swept airfoil, although carried out at relatively small Reynolds number, involve large angles of yaw within the boundary layer and therefore provide a useful test for the concept of vector similarity. In treating these data, incidentally, it has been assumed that the indication in some of the profiles of a sudden change in flow direction within the sublayer is fictitious.

The airfoil of Kuethe et al. was of elliptical plan form, of 18-inch chord and 96.5-inch span, with the major axis swept back at an angle of 25 degrees. Four profiles obtained near the trailing edge of the airfoil at an angle of attack of 14 degrees are plotted in Fig. 27 in terms of spanwise and chordwise components of mean velocity; in terms of streamwise and crossflow components; and finally in terms of wall and wake components.

The data in Fig. 27 can be fairly well represented by the characteristic wall and wake functions defined previously for unyawed flows, and it is difficult to say whether or not there is any systematic discrepancy. A more stimulating result, which may be coincidental or may illustrate an important intrinsic property of strongly wake-like yawed flows, is that the direction of the wake component is found in each case to be nearly the same as the direction of the gradient of the pressure field over the airfoil surface. That is, the final resolution is for practical purposes along the directions defined by the two vectors $\vec{\tau}_w$ and $-\text{grad } p$, so that $\text{grad } p \times \Pi \vec{\tau}_w$ vanishes everywhere. The inference that the constraint provided by inertia is also a vector constraint is

potentially useful in investigating the nature of the tensor parameter π when more suitable data become available from experiments carried out at larger Reynolds numbers in flow on a larger scale.

TABLE I

THE WAKE FUNCTION $w(\xi)$ AND RELATED FUNCTIONS

ξ	$w(\xi)$	$\frac{dw}{d\xi}$	$\int_0^w \xi dw$	$\omega_1(\Pi, \xi)$	$\omega_2(\Pi, \xi)$
0	0		0	$1 + 0.000 \Pi$	$1 + 0.000 \Pi + 0.000 \Pi^2$
.05	.004		0	$1 + 0.002 \Pi$	
.10	.029	.80	.002	$1 + 0.022 \Pi$	$1 + 0.027 \Pi + 0.000 \Pi^2$
.15	.084	1.38	.009	$1 + 0.062 \Pi$	
.20	.168	1.88	.024	$1 + 0.119 \Pi$	$1 + 0.154 \Pi + 0.008 \Pi^2$
.25	.272	2.29	.047	$1 + 0.190 \Pi$	
.30	.396	2.64	.082	$1 + 0.272 \Pi$	$1 + 0.360 \Pi + 0.044 \Pi^2$
.35	.535	2.88	.127	$1 + 0.363 \Pi$	
.40	.685	3.03	.183	$1 + 0.458 \Pi$	$1 + 0.614 \Pi + 0.127 \Pi^2$
.45	.838	3.10	.248	$1 + 0.552 \Pi$	
.50	.994	3.14	.322	$1 + 0.645 \Pi$	$1 + 0.880 \Pi + 0.257 \Pi^2$
.55	1.152	3.13	.405	$1 + 0.737 \Pi$	
.60	1.307	3.06	.495	$1 + 0.824 \Pi$	$1 + 1.143 \Pi + 0.426 \Pi^2$
.65	1.458	2.93	.589	$1 + 0.906 \Pi$	
.70	1.600	2.71	.685	$1 + 0.978 \Pi$	$1 + 1.380 \Pi + 0.610 \Pi^2$
.75	1.729	2.39	.778	$1 + 1.037 \Pi$	
.80	1.840	1.97	.863	$1 + 1.079 \Pi$	$1 + 1.561 \Pi + 0.765 \Pi^2$
.85	1.926	1.40	.935	$1 + 1.100 \Pi$	
.90	1.980	.73	.981	$1 + 1.090 \Pi$	$1 + 1.640 \Pi + 0.823 \Pi^2$
.95	1.999		.999	$1 + 1.051 \Pi$	
1.000	2.000		1.000	$1 + 1.000 \Pi$	$1 + 1.600 \Pi + 0.761 \Pi^2$

References

1. Nikuradse, J., Widerstandsgesetz und Geschwindigkeitsverteilung von turbulenten Wasserströmung in glatten und rauhen Röhren, Proc. 3rd Int. Cong. Appl. Mech., Stockholm, pp. 239-248, 1930.
2. Prandtl, L., Über die ausgebildete Turbulenz, Proc. 2nd Int. Cong. Appl. Mech., Zürich, pp. 62-74, 1926; translated as Turbulent flow, NACA TM 435, 1927.
3. von Kármán, T., Theorie des Reibungswiderstandes, Proc. Cong. on Hydromechanische Probleme des Schiffsantriebs, Hamburg, 1932.
4. Ludwig, H. and Tillmann, W., Untersuchungen über die Wandschubspannung in turbulenten Reibungsschichten, Ing.-Arch., Vol. 17, No. 4, pp. 288-299, 1949; translated as Investigations of the wall shearing stress in turbulent boundary layers, NACA TM 1285, 1950.
5. Clauser, F., Turbulent boundary layers in adverse pressure gradients, J. Aero. Sci., Vol. 21, No. 2, pp. 91-108, 1954.
6. Reichardt, H., Die Wärmeübertragung in turbulenten Reibungsschichten, Z.a.M.M., Vol. 20, No. 6, pp. 297-328, 1940; translated as Heat transfer through turbulent friction layers, NACA TM 1047, 1943.
7. Laufer, J., The structure of turbulence in fully developed pipe flow, NACA TN 2954, 1953.
8. Klebanoff, P., Characteristics of turbulence in a boundary layer with zero pressure gradient, NACA TN 3178, 1954.
9. Klebanoff, P. and Diehl, Z., Some features of artificially thickened fully developed turbulent boundary layers with zero pressure gradient, NACA TN 2475, 1951.
10. Coles, D., The problem of the turbulent boundary layer, Z.a.M.P., Vol. 5, No. 3, pp. 181-203, 1954.
11. Sheppard, P., The aerodynamic drag of the earth's surface and the value of von Kármán's constant in the lower atmosphere, Proc. Roy. Soc., A., Vol. 188, No. 1013, pp. 208-222, 1947.
12. Coles, D., The law of the wall in turbulent shear flow, 50 Jahre Grenzschichtforschung (ed. H. Görtler and W. Tollmien), F. Vieweg und Sohn, Braunschweig, pp. 153-163, 1955.
13. von Kármán, T., Über laminare und turbulente Reibung, Z.a.M.M., Vol. 1, No. 4, pp. 233-252, 1921; translated as On laminar and turbulent friction, NACA TM 1092, 1946.
14. Wieghardt, K., Über die Wandschubspannung in turbulenten Reibungsschichten bei veränderlichem Aussendruck, Z.W.B., K.W.I., Göttingen, U und M 6603, 1943. See also Wieghardt, K. and Tillmann, W., Zur turbulenten Reibungsschicht bei Druckanstieg, Z.W.B., K.W.I., Göttingen, U und M 6617, 1944; translated as On the turbulent friction layer for rising pressure, NACA TM 1314, 1951.

15. Wieghardt, K., Zum Reibungswiderstand rauher Platten, Z.W.B., K.W.I., Göttingen, U und M 6612, 1944.
16. Bauer, W., The development of the turbulent boundary layer on steep slopes, State Univ. of Iowa, Thesis, 1951; abridged in Proc. ASCE, Separate No. 281, 1953.
17. Schubauer, G. and Klebanoff, P., Investigation of separation of the turbulent boundary layer, NACA TN 2133, 1950.
18. Newman, B., Some contributions to the study of the turbulent boundary layer near separation, Austr. Dept. Supply, Rep. No. ACA-53, 1951.
19. Kehl, A., Untersuchungen über konvergente und divergente turbulente Reibungsschichten, Ing.-Arch., Vol. 13, No. 5, pp. 293-329, 1943; translated as Investigations on convergent and divergent turbulent boundary layers, British R.T.P. No. 2035, 1946.
20. McCullough, G. and Gault, D., Boundary-layer and stalling characteristics of the NACA 64A006 airfoil section, NACA TN 1923, 1949.
21. Tillmann, W., Untersuchungen über Besonderheiten bei turbulenten Reibungsschichten an Platten, Z.W.B., K.W.I., Göttingen, U und M 6627, 1945; translated as Investigations of some particularities of turbulent boundary layers on plates, British R and T MAP-VG-34, 1946.
22. Millikan, C., A critical discussion of turbulent flows in channels and circular tubes, Proc. 5th Int. Cong. Appl. Mech., Cambridge, pp. 386-392, 1938.
23. Von Doenhoff, A. and Tetervin, N., Determination of general relations for the behavior of turbulent boundary layers, NACA TR 772, 1943.
24. Gruschwitz, E., Die turbulente Reibungsschicht in ebener Strömung bei Druckabfall and Druckanstieg, Ing.-Arch., Vol. 2, No. 3, pp. 321-346, 1931.
25. Liepmann, H. and Laufer, J., Investigations of free turbulent mixing, NACA TN 1257, 1947.
26. Tillmann, W., Über die Wandschubspannung turbulenter Reibungsschichten bei Druckanstieg, Thesis, Göttingen, 1947.
27. Lees, L. and Crocco, L., A mixing theory for the interaction between dissipative flows and nearly isentropic streams, J. Aero. Sci., Vol. 19, No. 10, pp. 649-676, 1952.
28. Ross, D. and Robertson, J., A superposition analysis of the turbulent boundary layer in an adverse pressure gradient, J. Appl. Mech., Vol. 18, pp. 95-100, 1951.
29. Rotta, J., Über die Theorie der turbulenten Grenzschichten, Mitt. M.-P.-Inst., Göttingen, No. 1, 1950; translated as On the theory of the turbulent boundary layer, NACA TM 1344, 1953.

30. Korkegi, R., Transition studies and skin friction measurements on an insulated flat plate at a hypersonic Mach number, GALCIT Hypersonic Wind Tunnel Memo. No. 17, 1954.
31. Gruschwitz, E., Turbulente Reibungsschichten mit Sekundärströmung, Ing.-Arch., Vol. 6, No. 5, pp. 355-365, 1935.
32. Kuethe, A., McKee, P., and Curry, W., Measurements in the boundary layer of a yawed wing, NACA TN 1946, 1949.

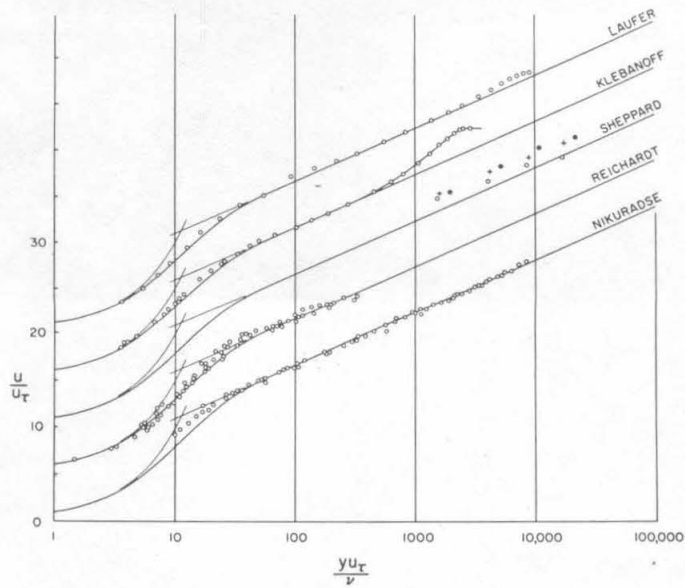


Fig. 1. The Law of the Wall

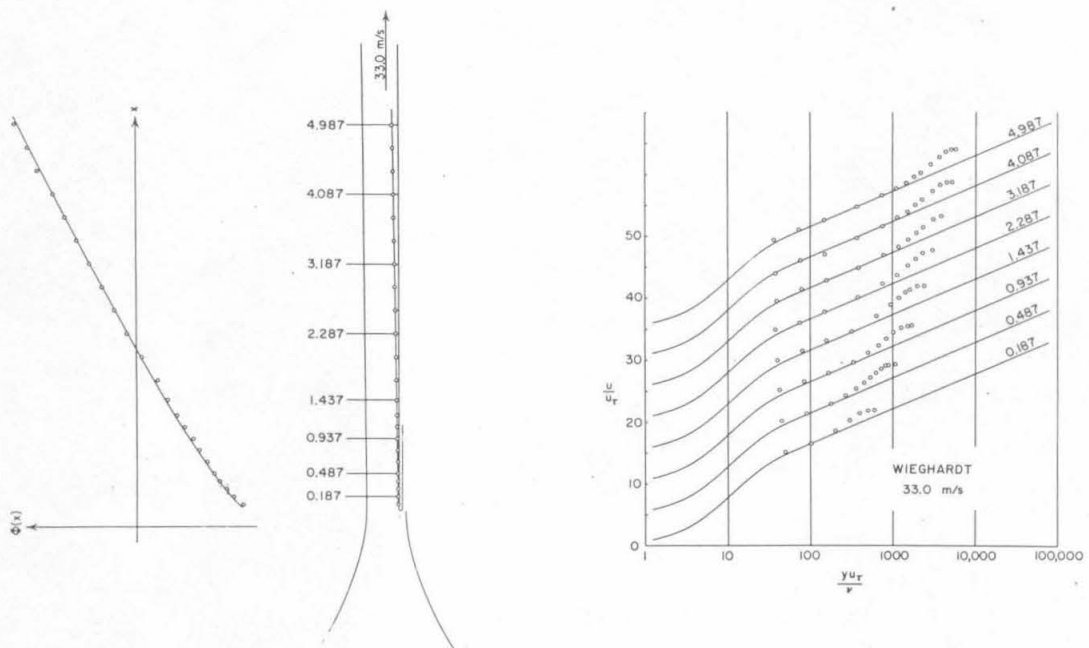


Fig. 2. Data of Wieghardt¹⁴ for Constant Stream Velocity

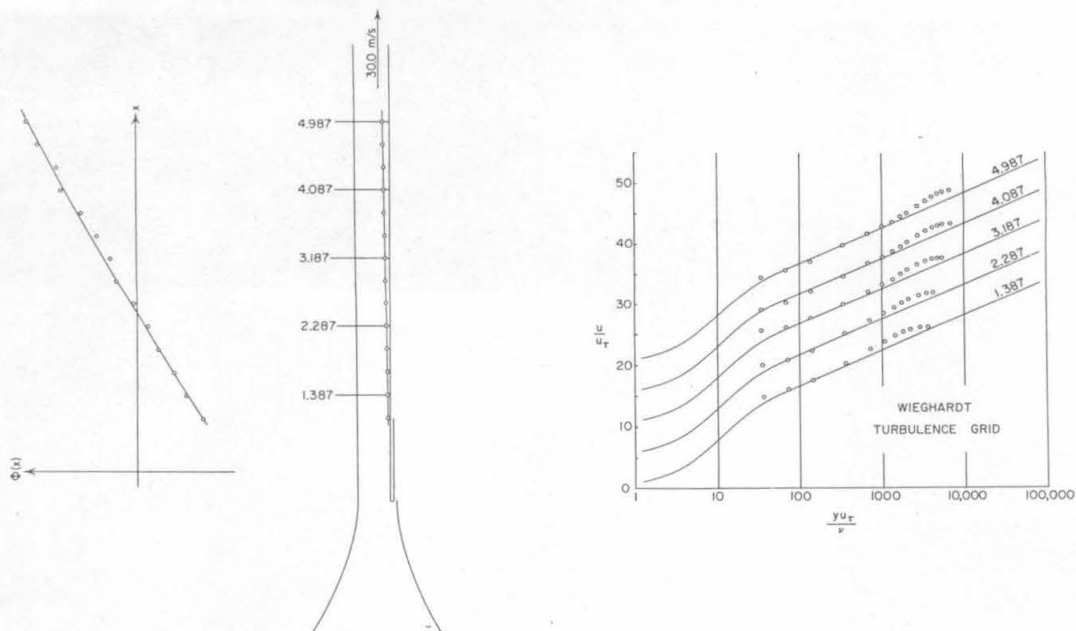


Fig. 3. Data of Wieghardt¹⁵ with Turbulence Grid

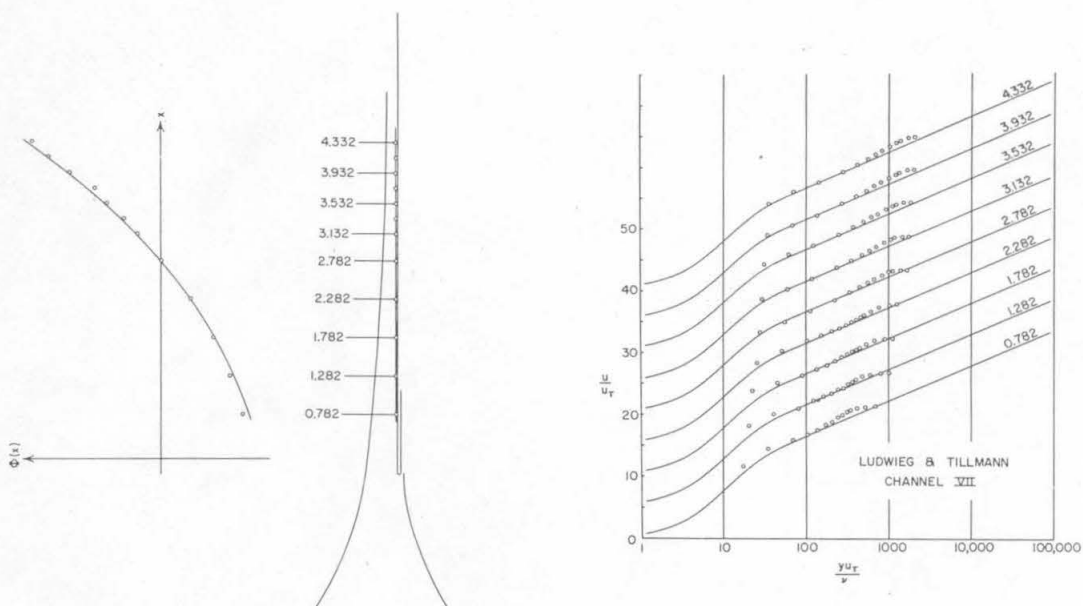


Fig. 4. Data of Ludwig and Tillmann⁴ for Falling Pressure

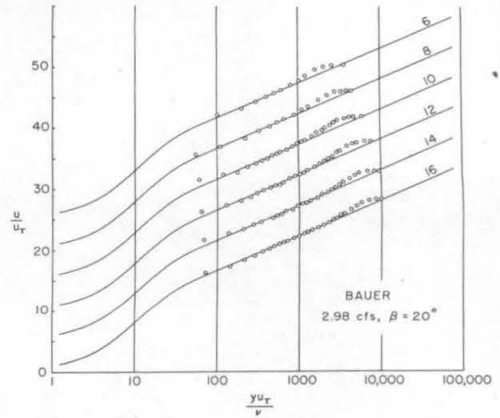
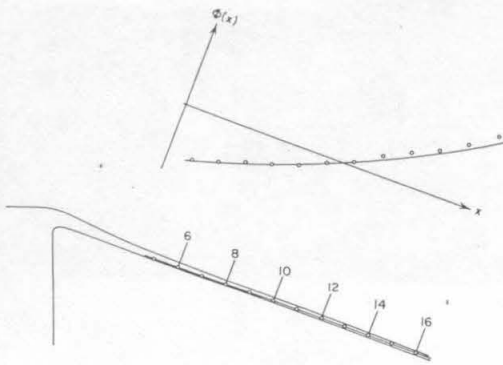


Fig. 5. Data of Bauer¹⁶ for 20° Slope

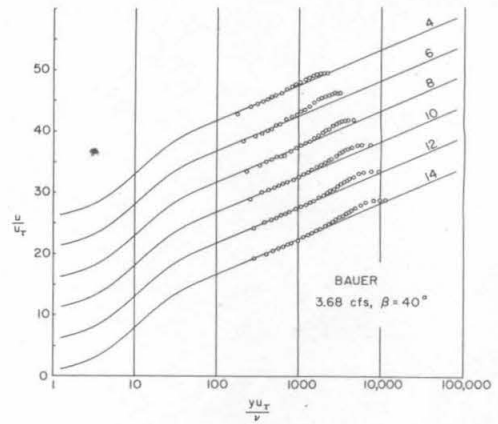
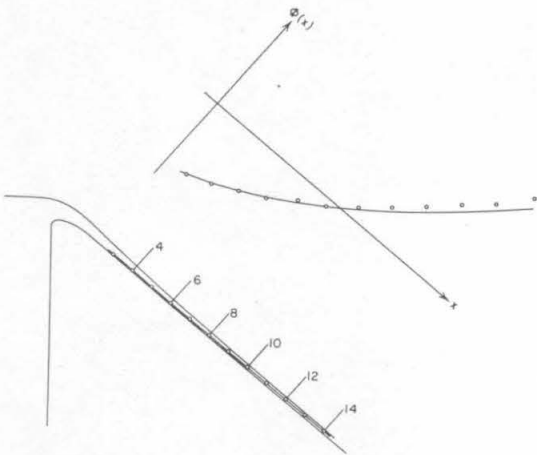


Fig. 6. Data of Bauer¹⁶ for 40° Slope

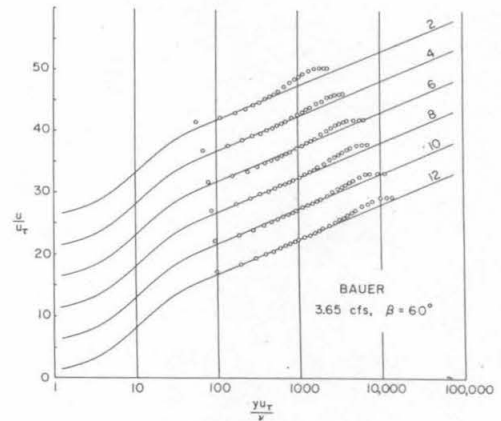
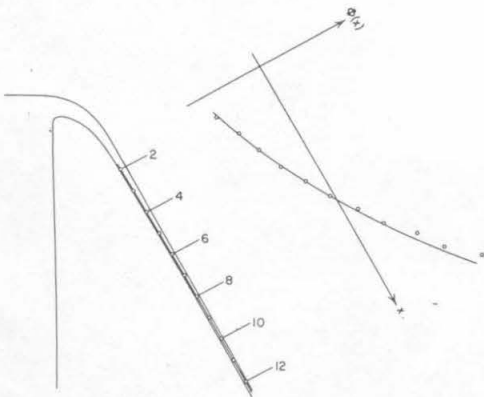


Fig. 7. Data of Bauer¹⁶ for 60° Slope

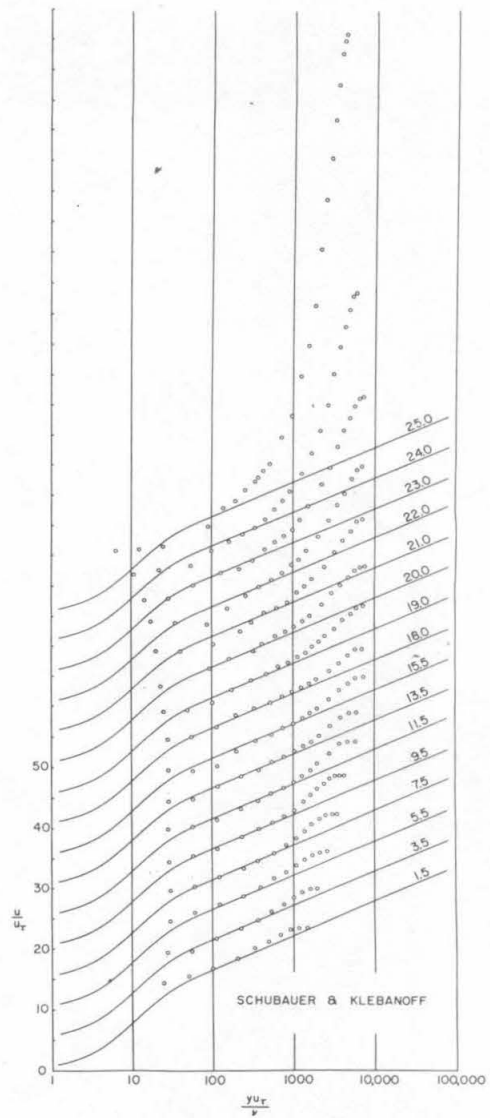
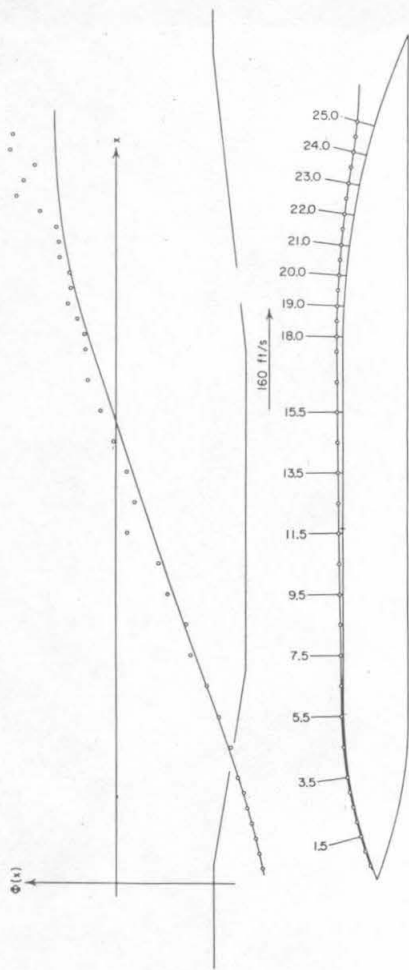


Fig. 8. Data of Schubauer and Klebanoff¹⁷

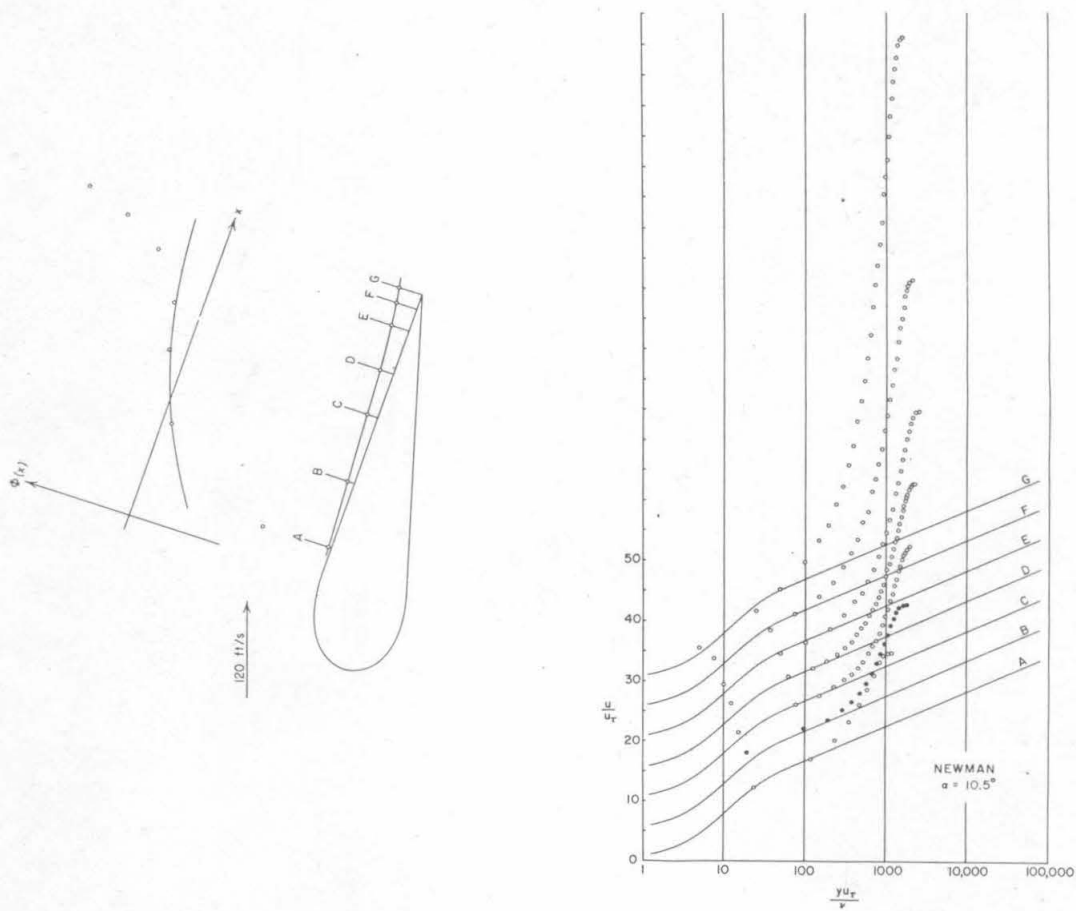


Fig. 9. Data of Newman¹⁸

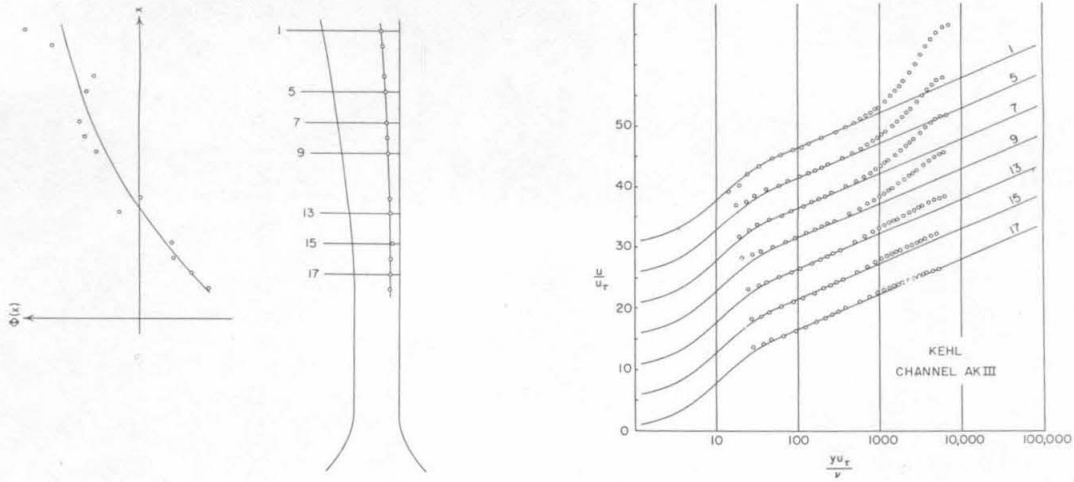


Fig. 10. Data of Kehl¹⁹

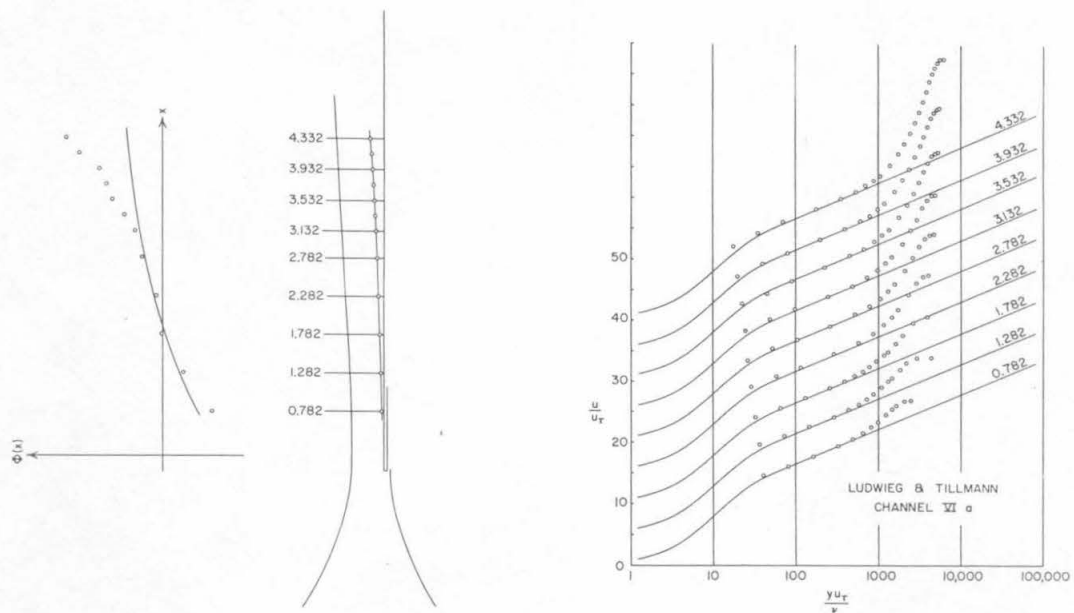


Fig. 11. Data of Ludwig and Tillmann⁴ for Moderately Rising Pressure

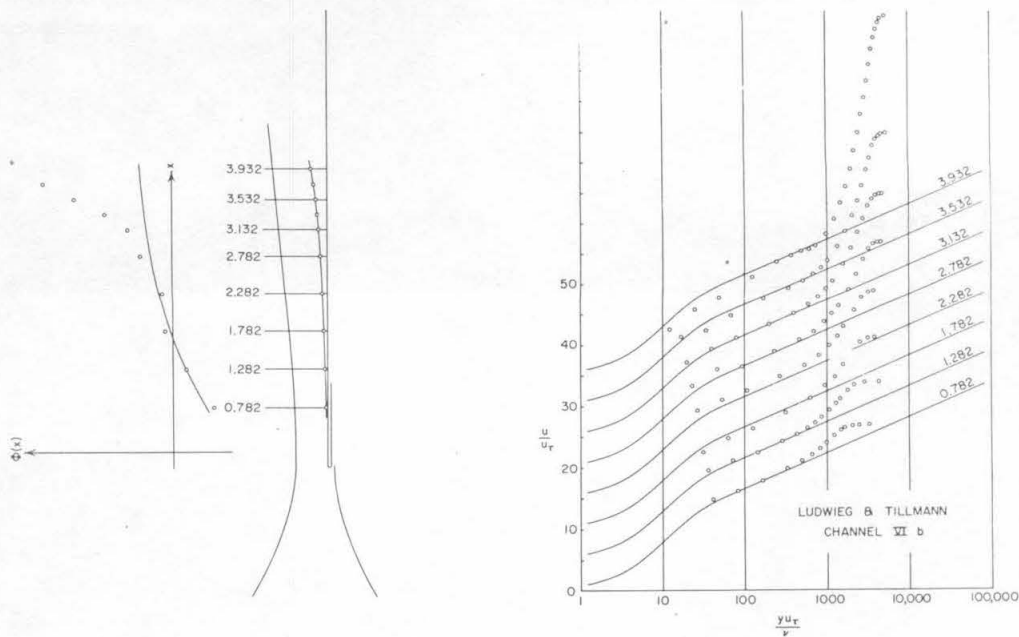


Fig. 12. Data of Ludwig and Tillmann⁴ for Strongly Rising Pressure

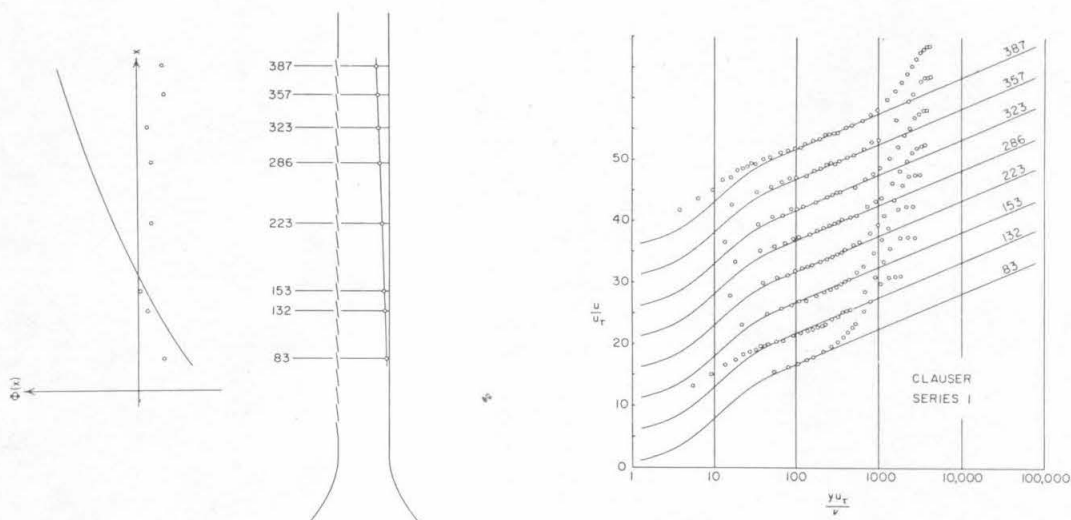


Fig. 13. Data of Clauser⁵ for Moderately Rising Pressure

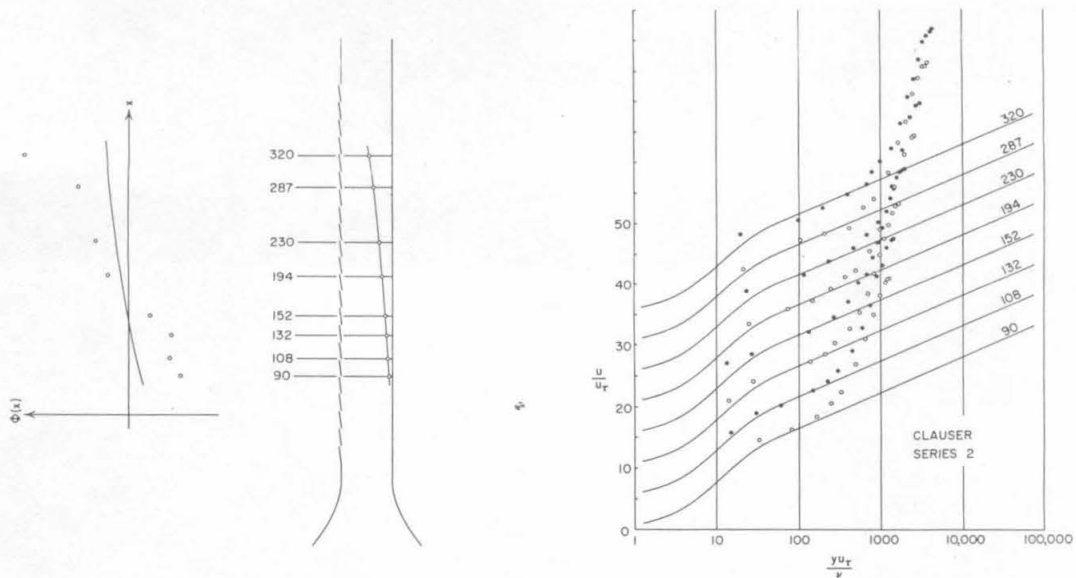


Fig. 14 Data of Clauser⁵ for Strongly Rising Pressure

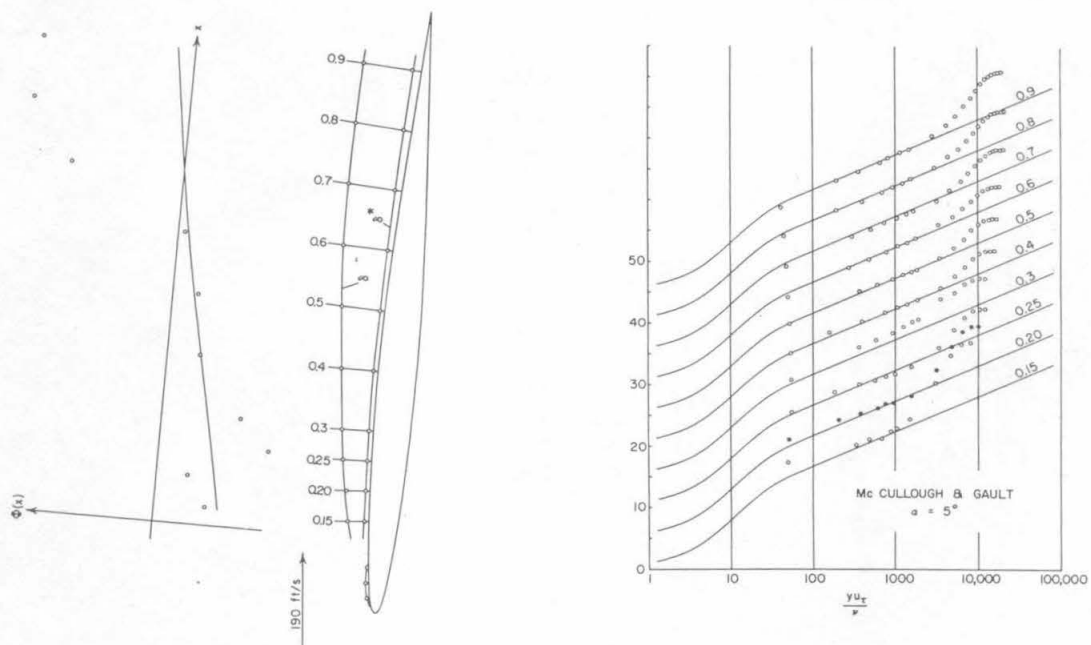


Fig. 15. Data of McCullough and Gault²⁰ for 5° Angle of Attack

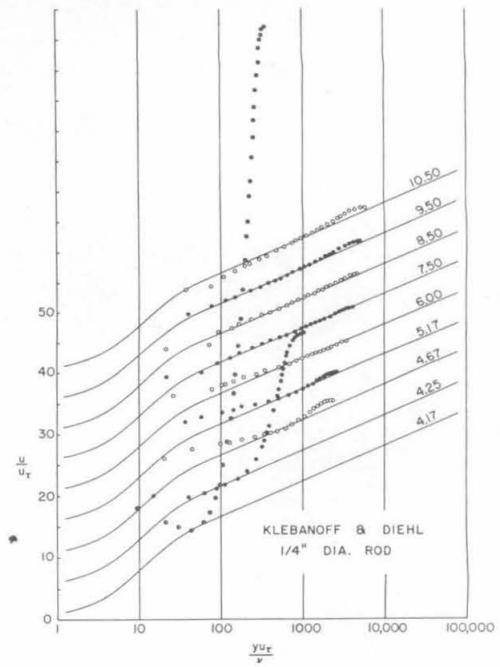
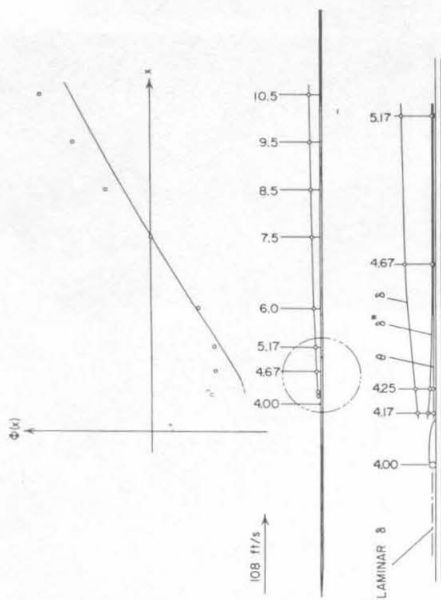


Fig. 16. Data of Klebanoff and Diehl⁹ for 1/4-inch Rod

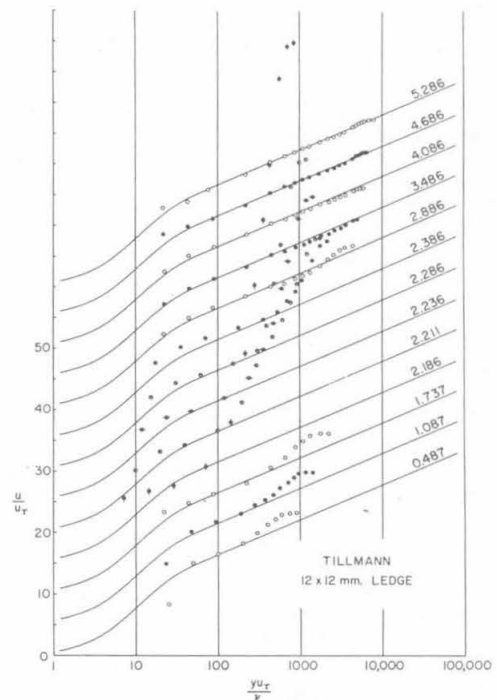


Fig. 17. Data of Tillmann²¹ for 12-mm. Ledge

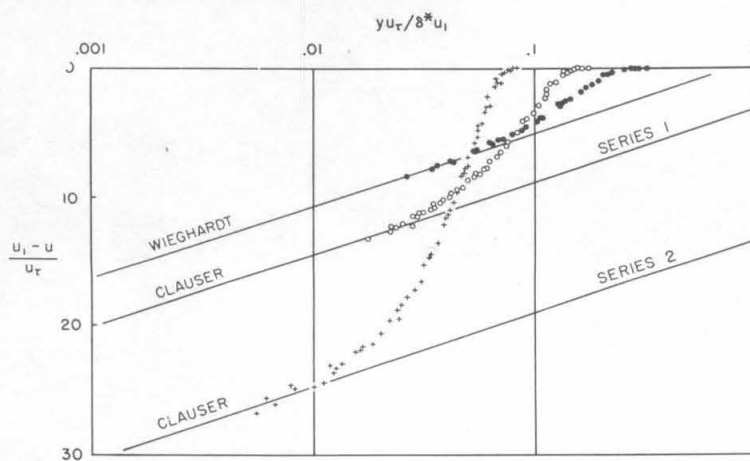


Fig. 18. The Defect Law

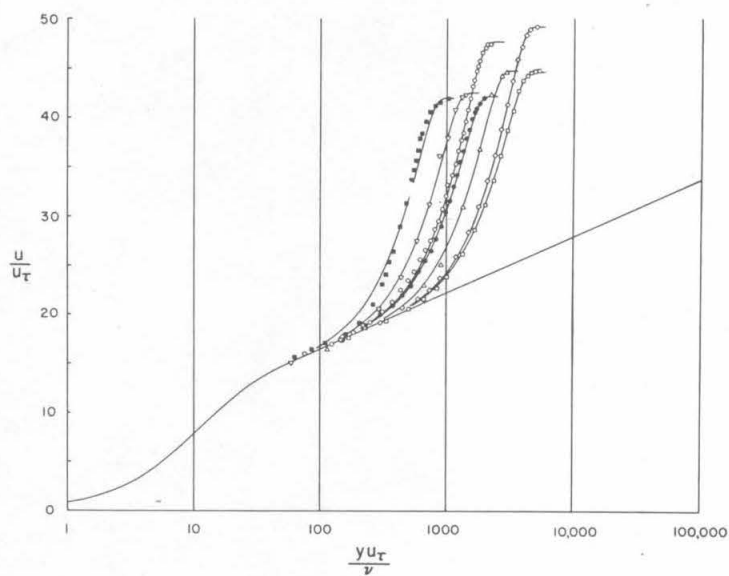


Fig. 19. Two-Parameter Similarity in the Mean-Velocity Profile

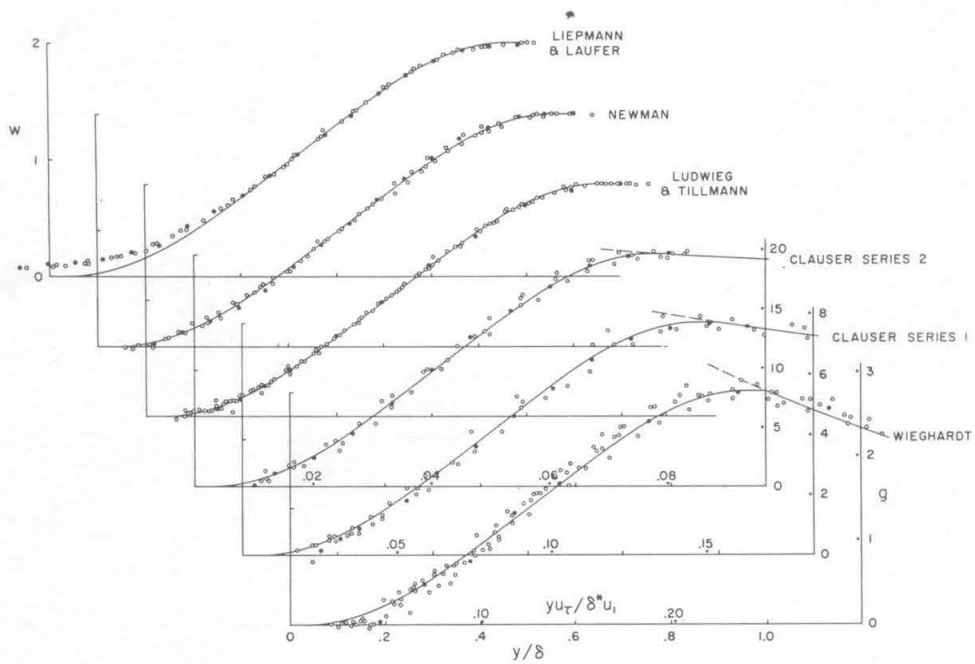


Fig. 20. The Law of the Wake

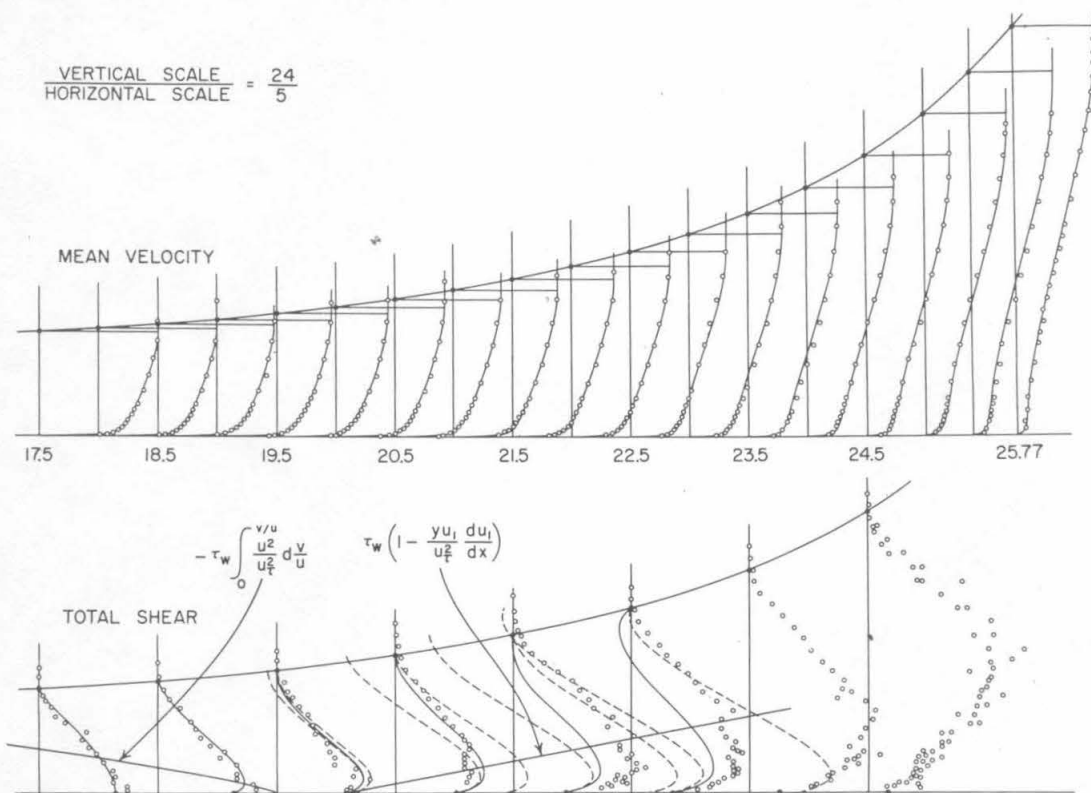


Fig. 21. The Separating Flow of Schubauer and Klebanoff¹⁷ (Measured values of shear have been reduced by 31 percent)

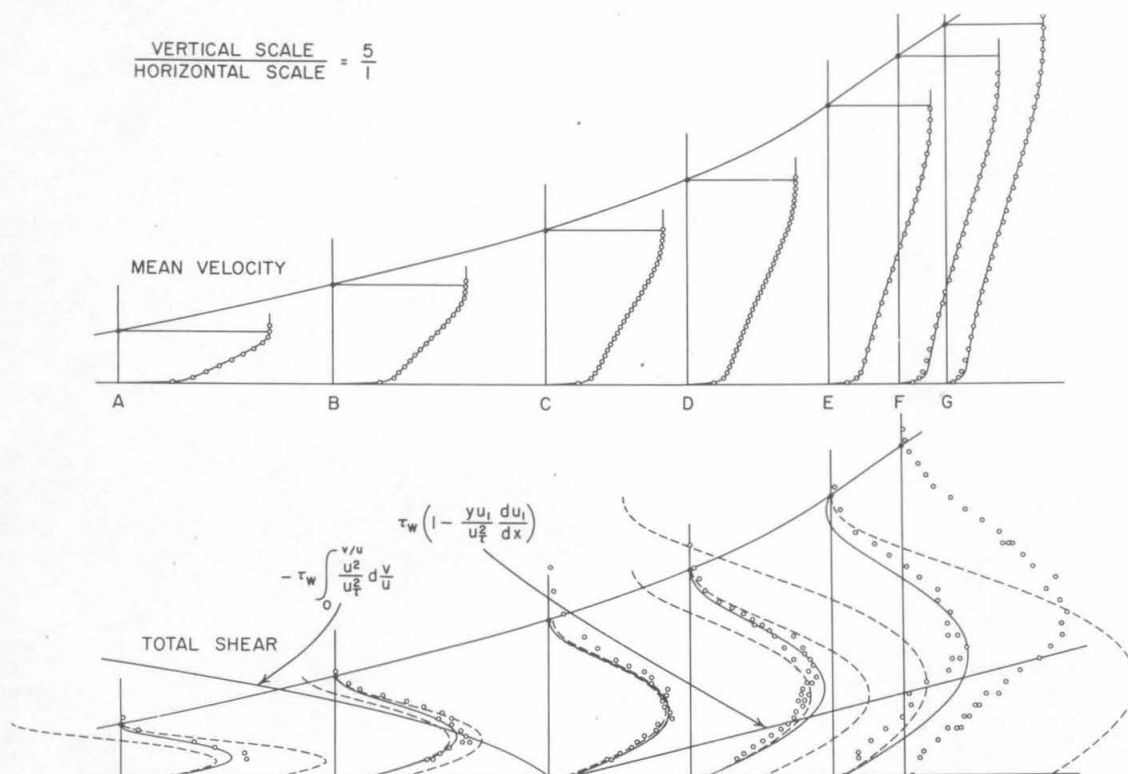


Fig. 22. The Separating Flow of Newman¹⁸

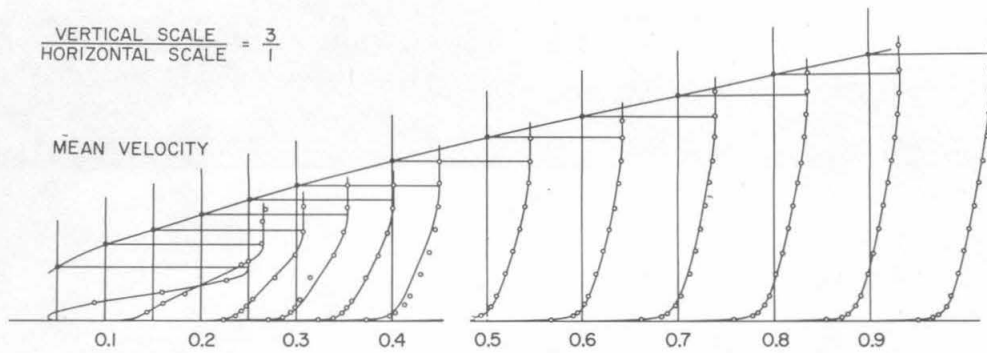


Fig. 23. The Reattaching Flow of McCullough and Gault²⁰

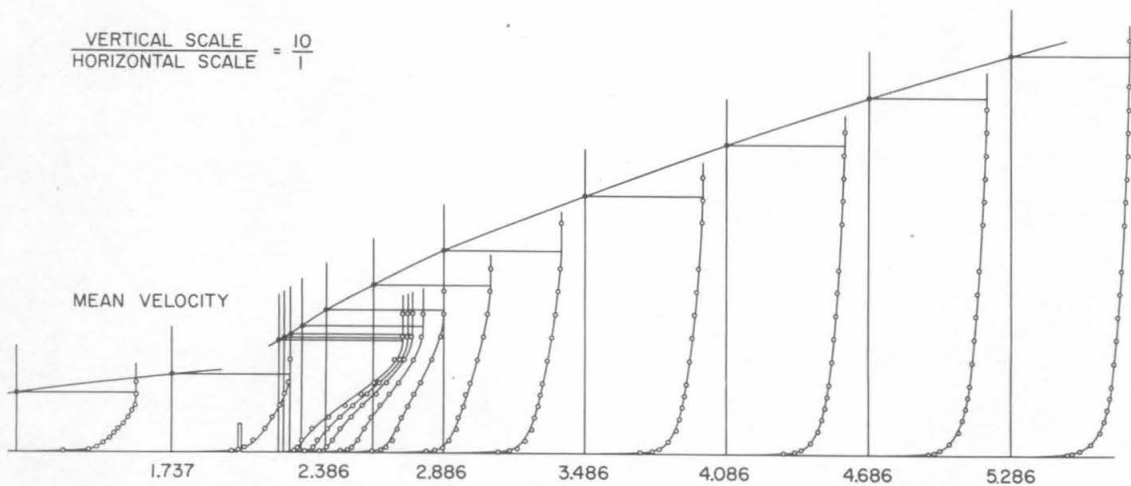


Fig. 24. The Reattaching Flow of Tillmann²¹

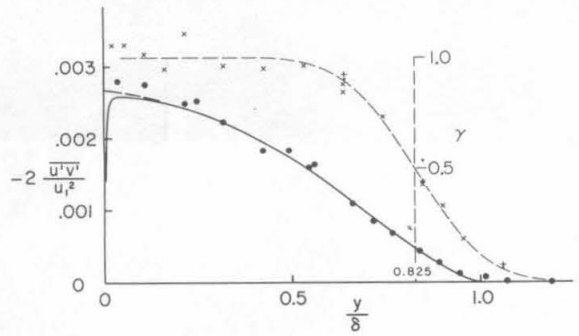


Fig. 25. Shear Profile in the Flow of Klebanoff⁸

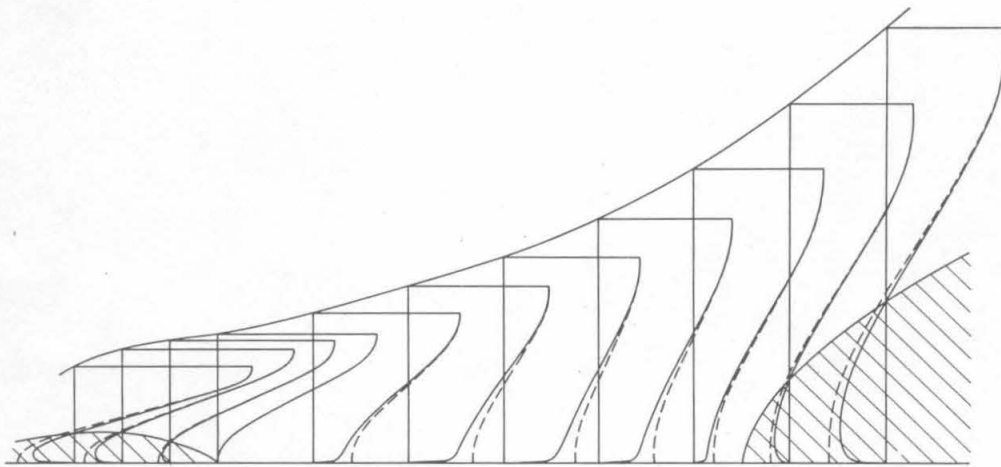


Fig. 26. Hypothetical Boundary Layer Showing the Equivalent Wake

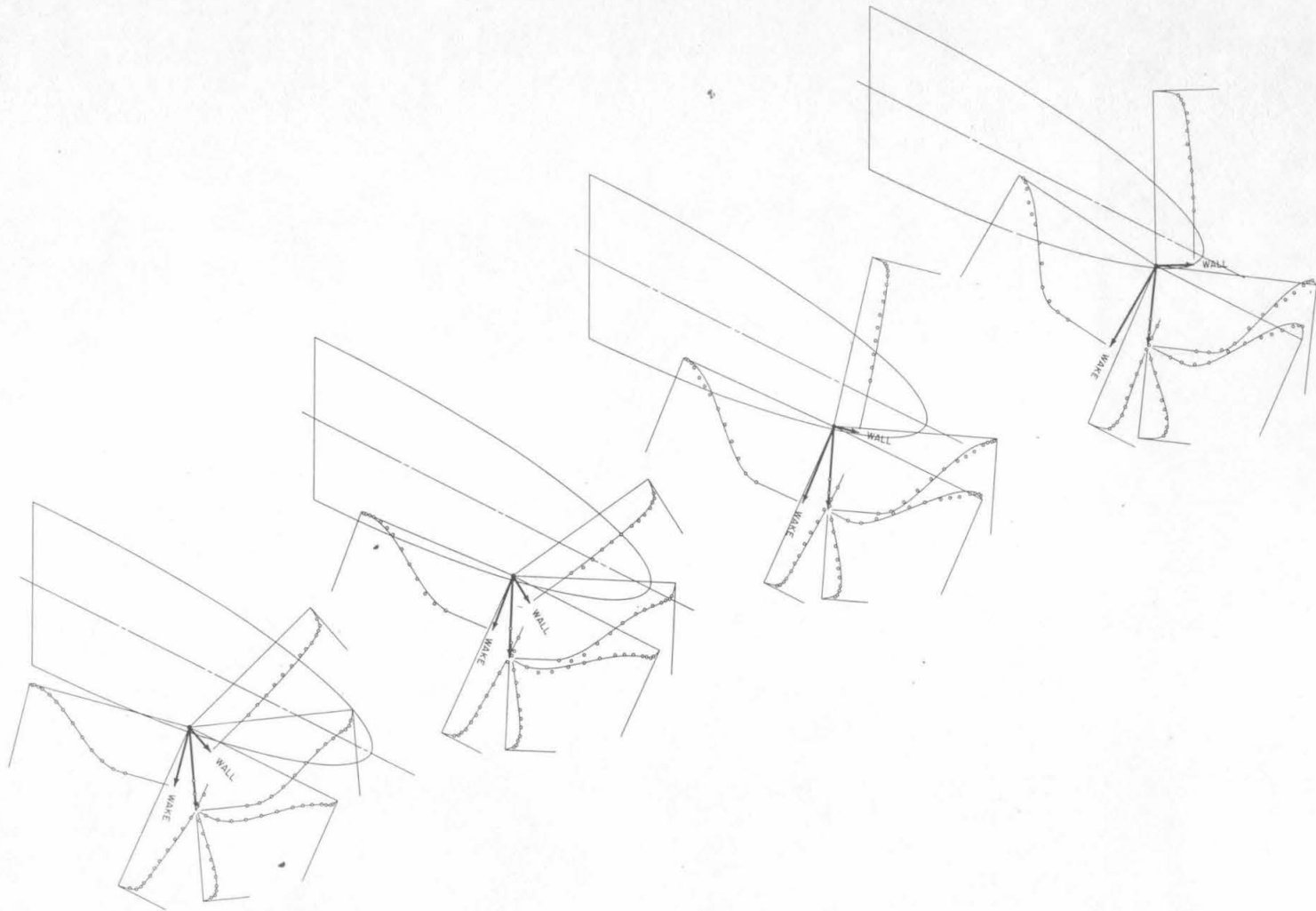


Fig. 27. Vector Resolution of the Yawed Flow of Kuethe, McKee, and Curry³²